

Consistent Pricing of Options on Leveraged ETFs

Andrew Ahn

Department of IE and OR, Columbia University, New York, NY 10027, aja2133@columbia.edu.

Martin Haugh

Department of IE and OR, Columbia University, New York, NY 10027, mh2078@columbia.edu.

Ashish Jain

ashish.jain@us.bnpparibas.com

Latest draft: October 2014

Abstract

We consider the problem of pricing options on a leveraged ETF (LETF) and the underlying ETF in a consistent manner. We show that if the underlying ETF has Heston dynamics then the LETF also has Heston dynamics so that options on both the ETF and the LETF can be priced analytically using standard transform methods. If the underlying ETF has tractable jump-diffusion dynamics then the dynamics of the corresponding LETF are generally intractable in that we cannot compute a closed-form expression for the characteristic function of the log-LETF price. In that event we propose tractable approximations based on either moment-matching techniques or saddlepoint approximations to the LETF price dynamics under which the characteristic function of the log-LETF price can be found in closed form. In a series of numerical experiments including both low and high volatility regimes, we show that the resulting LETF option price approximations are very close to the true prices which we calculate via Monte-Carlo. Because approximate LETF option prices can be computed very quickly our methodology should be useful in practice for pricing and risk-managing portfolios that contain options on both ETFs and related LETFs. Our numerical results also demonstrate the model-dependency of LETF option prices and this is particularly noticeable in high-volatility environments.

1 Introduction

According to various industry sources, there were more than 4,500 registered ETFs globally in 2010 with assets under management (AUM) of approximately \$1.6 trillion. These ETFs are spread among many asset classes including equity, fixed income, commodity and FX. There were liquid options available on approximately 400 of these ETFs in 2010 and these ETFs accounted for approximately \$1 trillion of the \$1.6 trillion in AUM. Moreover the total ETF options volume is very large indeed: according to the Chicago Board Options Exchange [8], of the 4 billion exchange traded options contracts in 2010, 1.3 billion were ETF options, with equity options and cash index options accounting for 2.4 billion and 0.3 billion, respectively. In contrast, there were approximately 2 billion contracts traded in 2006, with a split of 1.5 billion equity options, 350 million ETF options and 180 million cash index options. Between 2006 and 2010 the ETF options market therefore grew by a factor of four and is now a very large market indeed.

An even more recent development has been the introduction of *leveraged* ETFs (LETFs). An LETF is an exchange-traded derivative security based on a single underlying ETF or index. It is intended to achieve a *daily* return of ϕ times the daily return of the underlying ETF and the LETF manager needs to re-balance his portfolio on a daily basis in order to achieve this. The constant ϕ is known as the *leverage ratio* of the LETF. As of 2010, there were approximately 150 LETFs with a total of \$30 billion in AUM and approximately 100 of these LETFs have liquid options traded on them. Moreover, a given LETF typically has a very large and liquid ETF or index as its underlying security with options traded on both the LETF and the underlying ETF.

Upon their introduction, there was considerable confusion among investors over the performance of LETFs, particularly during the financial crisis when volatility levels spiked to unprecedented levels. In particular, many investors did not appreciate that LETFs had a negative exposure to the realized variance of the underlying ETF and therefore did not anticipate their potentially poor performance during this period. Cheng and Madhavan [6] and Avellaneda [2] were the first to model and explain this LETF performance. In a continuous-time diffusion framework they obtained an expression (see (2) below) that highlighted this negative exposure to realized variance. Based on results in Haugh and Jain [13], Haugh [12] also derived this expression as a simple case of a more general expression for the realized wealth that results from following a constant proportion trading strategy in a multi-security diffusion setting.

While these papers helped to explain LETF performance, there has been little work on the pricing of LETF options and, in particular, on pricing them in a manner that is *consistent* with the pricing of options on the underlying ETF. One approach for pricing LETF options is based on using the Black-Scholes formula with the implied volatility taken from a related ETF option and then scaled by the leverage ratio. But this approach is ad-hoc and has not been properly justified. Concurrent with our work is the recent paper of Leung and Sircar [15] who use asymptotic techniques in a diffusion setting to understand the link between implied volatilities of the underlying ETF and related LETFs of a given leverage ratio. They then use the resulting insights to identify possible mispricings in the market-place.

In this paper we price LETF options quickly and *consistently* with options on the underlying ETF under three different models: (i) Heston's [14] stochastic volatility model (ii) the Bates [4] jump-diffusion model and (iii) an affine jump-diffusion (AJD) model of Duffie, Pan and Singleton [7]

which includes jumps in both the volatility and price processes. In the sequel we will often refer to these models as the SV, SVJ and SVCJ models, respectively. It should also be clear that the approximation techniques we develop in this paper can be applied more generally and that our treatments of the SV, SVJ and SVCJ models may be viewed as applications of a more general approach. For example, other AJD models of Duffie et al. [7] should also be amenable to our approximation techniques. We do not propose a “one-size-fits-all” approximation, however, so some additional work will generally be required to obtain a suitable approximation for a new set of underlying ETF price dynamics.

We show that if the underlying ETF has Heston dynamics then the LETF also Heston dynamics so that options on both the ETF and the LETF can be priced analytically using standard transform methods. If the underlying ETF has tractable jump-diffusion dynamics (as in (ii) and (iii) above) then the dynamics of the corresponding LETF are generally intractable in that we cannot compute a closed-form expression for the characteristic function of the log-LETF price. Instead we can either compute this characteristic function numerically (as in (ii) above) or else (as in (iii) above) we construct tractable approximations to the LETF dynamics where the characteristic function of the log-LETF price can be found in closed form. Such approximations enables us to calculate approximate option prices very quickly. The key to this latter approach is that under our jump-diffusion models for the underlying ETF, the diffusion component of the LETF dynamics remains “tractable”. We therefore only need to focus on approximating the jump component of the LETF dynamics.

The approximations that we propose include¹ classic moment-matching techniques and the saddlepoint approximation approach of Glasserman and Kim [9] for handling less tractable affine jump diffusion processes. In a series of numerical experiments including both low and high volatility regimes, we show that the resulting LETF option price approximations are very close to the true prices which we calculate via Monte-Carlo. Our approximate LETF option prices can be computed quickly and therefore should be useful in practice for pricing and risk-managing portfolios that contain options on both ETFs and related LETFs.

Our numerical experiments also show that the ratio of an LETF option implied volatility to the corresponding ETF option implied volatility can be far from the LETF leverage ratio. The difference between the two depends on whether or not the LETF is long or short and is model dependent, thereby emphasizing the path dependence of the LETF price at any given time. In order to illustrate just how model dependent the prices of LETF options can be, we also price these options under the Barndorff-Nielsen and Shephard [3] model in addition to the three models listed above. This model dependency calls into question the market practice of pricing an LETF option using the Black-Scholes formula with the strike and implied volatility scaled by the leverage ratio.

Finally, it is worth emphasizing that our use of the word “consistent” in the title of this paper refers to *model* or *internal* consistency. In particular, rather than using separate models for pricing ETF options and LETF options our goal is to show how to consistently price these options at the model

¹Earlier versions of this paper proposed an approach where the entire distribution of the jump component of the LETF price dynamics was approximated by a more tractable distribution. While the resulting approximations were very accurate the approach was very ad-hoc and somewhat awkward to describe. We have therefore replaced it with approaches based on moment-matching and saddlepoint approximations. While both of these new approaches also require some work to implement, they are less ad-hoc, easier to describe and, as standard approximation techniques, they are easy to justify.

level only. We therefore do not claim that any one model can always price these options consistently with market prices. Indeed given the behavior of financial markets, we expect that the only models capable of always fitting to market prices are those models which have too many parameters and therefore tend to over-fit. Moreover, given the need to frequently re-calibrate even parsimonious models throughout the derivatives markets, we suspect that such models may never be found.

The remainder of this paper is organized as follows. Section 2 describes our modeling assumptions for LETF price dynamics. In Sections 3, 4 and 5 we consider the SV, SVJ and SVCJ models, respectively, for the underlying ETF and describe how LETF options can be calculated for each of these models. Section 6 describes how we calibrated these models and Section 7 provides numerical results confirming the quality of our moment-matching approximation for the SVCJ model. We describe the saddlepoint approximation approach in Section 8 and we conclude in Section 9. The appendices contain further details on our approximation methods as well as some additional numerical results. Our comments in the previous paragraph notwithstanding, in Appendix D we provide a snapshot of how these models perform when they have been calibrated to market data. In particular, we will compare the model prices of LETF options with the corresponding market prices when the models have been calibrated to the market prices of ETF options. We will see that (at least on the day in question) the calibrated models produced very accurate prices for LETF options.

2 Modeling Leveraged ETF Dynamics

We let S_t and L_t denote the time t prices of the underlying ETF and LETF, respectively. Rather than working in discrete time we will work instead in continuous-time and assume that the LETF is re-balanced continuously.

Modeling Leveraged ETF Dynamics When the Underlying Has Diffusion Dynamics

If S_t follows a diffusion then the mechanics of the LETF implies that L_t has dynamics

$$\frac{dL_t}{L_t} = \phi \cdot \frac{dS_t}{S_t} + (1 - \phi)r dt - f dt \quad (1)$$

where r is the continuously compounded risk-free interest rate and f is the constant expense ratio of the LETF. There is no difficulty incorporating dividends as long as we interpret the dS_t term in (1) to include any dividend payments. The $(1 - \phi)r dt$ term in (1) reflects the cost of funding the leveraged position when $\phi > 1$, or the risk-free income from an inverse ETF when $\phi < 0$.

Assuming general diffusion dynamics of the form $dS_t = \mu_t S_t dt + \sigma_t S_t dW_t$, Avellaneda and Zhang [2] solved² (1) to obtain

$$\frac{L_T}{L_0} = \left(\frac{S_T}{S_0} \right)^\phi \exp \left((1 - \phi)rT - fT + \frac{1}{2}\phi(1 - \phi) \int_0^T \sigma_t^2 dt \right). \quad (2)$$

They used this expression to explain the empirical performance of LETFs during the financial crisis. Note that for leverage ratios satisfying $|\phi| > 1$ it is clear from (2) that a long LETF position is short

²Cheng and Madhavan [6] obtained (2) under geometric Brownian motion dynamics.

realized variance for a given value of S_T . Haugh and Jain [13] also derived a more general form of (2) in a dynamic portfolio optimization context. It is also easy to show that this negative exposure to variance could be interpreted as a (multiplicative) premium that must be paid for obtaining a payoff of $(S_T/S_0)^\phi$ rather than the payoff you would obtain from a buy-and-hold portfolio with initial leverage of ϕ .

Modeling Leveraged ETF Dynamics When the Underlying Can Jump

Note also that if S_t can jump then (1) will still be valid as long as we truncate the jumps appropriately to reflect the limited liability of the LETF. But of course the LETF manager must implicitly pay for the truncation of these jumps since otherwise an arbitrage opportunity would exist. When the underlying price process can jump we therefore assume dynamics for L_t of the form

$$\frac{dL_t}{L_{t-}} = \phi \cdot \frac{dS_t^*}{S_{t-}} + (1 - \phi)rdt - fdt - c_t dt \quad (3)$$

where dS_t^* denotes the possibly truncated increment in the underlying price at time t and $c_t dt$ is the “insurance premium” paid at time t to insure against L_t violating limited liability in the next dt units of time. Note that we can also write (3) more explicitly as

$$\frac{dL_t}{L_{t-}} = \phi \cdot \frac{dS_t}{S_{t-}} + (1 - \phi)rdt - fdt - c_t dt \quad \text{for } 0 \leq t < \tau \quad (4)$$

where τ is the first-passage time of the event $\phi dS_t/S_{t-} \leq -1$. Moreover we assume $L_t \equiv 0$ for all $t \geq \tau$.

2.1 Risk-Neutral Dynamics for the Leveraged ETF

While not stated explicitly, the dynamics in (1) to (4) are assumed to hold under P , the objective or true data-generating probability measure. Because these are pathwise dynamics they must therefore hold under any equivalent martingale measure, Q . In this paper we will take Q to be the martingale measure associated with taking the cash account as numeraire. We will also assume that the risk-free rate, r , is a constant³ but note that it would be straightforward to relax this assumption if necessary. Note that once we specify Q -dynamics for S_t we are also implicitly specifying Q -dynamics for L_t via (3) and (4).

All of our examples in this paper will assume that the underlying security price has risk-neutral dynamics of the form

$$\frac{dS_t}{S_{t-}} = (r - q - \lambda m)dt + \sqrt{V_t}dW_t^S + dJ_t, \quad (5)$$

where q is the dividend yield, λ is the intensity of the jump process, J_t , and V_t is some stochastic volatility process. We will write $J_t := \sum_{i=1}^{N_t} (Y_i - 1)$ so that $Y_i - 1$ represents the relative jump size in the security price at the time of the i^{th} jump. In particular, if the i th jump occurs at time τ_i , then $S_{\tau_i} = S_{\tau_i-} Y_i$. We set $m = \mathbb{E}^Q(Y_i - 1)$ which guarantees that the discounted gains process associated with holding the underlying security is a Q -martingale.

³Given the short expirations that are typical for LETF options the assumption of constant interest rates is easy to justify.

Some simple algebra confirms that jumps, Y_i , in the underlying security that satisfy $\phi(Y_i - 1) < -1$ would cause L_t to go negative in the absence of limited liability. In the presence of limited liability we must therefore use a jump process for L_t of the form, $J_t^L := \sum_{i=1}^{N_t} (Y_i^L - 1)$ where

$$Y_i^L := \max(\phi(Y_i - 1), -1) + 1.$$

Continuing our insurance analogy, we could imagine the leveraged ETF manager being exposed to all jumps, $\phi(Y_i - 1)$, but in such a way that he is insured against any jumps that would cause L_t to go negative. We can calculate the premium per unit time, c_t , as the (risk-neutral) expected loss per unit time that the insurer would incur due to a possible jump in L_t to a negative value. The risk-neutral value of this insurance⁴ is then given by

$$\begin{aligned} c_t &:= \lambda p^* (\mathbb{E}^Q[-1 - \phi(Y_i - 1) | \phi(Y_i - 1) < -1]) \\ &= -\lambda p^* (\mathbb{E}^Q[\phi(Y_i - 1) | \phi(Y_i - 1) < -1] + 1) \end{aligned} \quad (6)$$

where $p^* := Q(\phi(Y_i - 1) < -1)$ so that λp^* is the arrival rate for jumps that will drive L_t to zero. The “+1” term on the right-hand-side of (6) is required because the insurance only covers that part of the jump *beyond* -1 and indeed the jump event itself will drive the LETF price, L_t , to 0. Substituting (6) and (5) into (4) and also taking the insurance payoff, dJ_t^{ins} say, into account we obtain the following risk-neutral dynamics for L_t

$$\frac{dL_t}{L_t} = \phi \left((r - q - \lambda m)dt + \sqrt{V_t}dW_t^S + dJ_t \right) + (1 - \phi)r dt - f dt - c_t dt + dJ_t^{ins} \quad (7)$$

$$\begin{aligned} &= (r - \phi q - f - \lambda \phi m)dt + \phi \sqrt{V_t}dW_t^S + dJ_t^L - c_t dt \\ &= (r - \phi q - f - \lambda m_L)dt + \phi \sqrt{V_t}dW_t^S + dJ_t^L \end{aligned} \quad (8)$$

where we have used the fact that $\phi dJ_t + dJ_t^{ins} = dJ_t^L$ and used (6) and $m = \mathbb{E}^Q(Y_i - 1)$ to obtain

$$\begin{aligned} m_L &:= \phi m + c_t / \lambda \\ &= (1 - p^*) \cdot \mathbb{E}^Q[\phi(Y_i - 1) | \phi(Y_i - 1) > -1] - p^*. \end{aligned} \quad (9)$$

Note that these dynamics are only valid for $0 \leq t \leq \tau$ and that (7) does not contradict (4) since the dJ_t^{ins} term (which is absent in (4)) is only non-zero at time τ .

In the foregoing analysis we have implicitly assumed that dividends from the underlying ETF (or index) will be multiplied by ϕ and then paid out, in the case where ϕ is positive, to investors in the corresponding LETF. If ϕ is negative then the LETF investor will have to pay out these dividends. We make this assumption in order to simplify the exposition but note that in practice the treatment of dividends can vary with each LETF. For example, inverse LETFs with $\phi < 0$ typically have a dividend yield of zero and do not require their investors to make dividend payments while positively leveraged ETFs typically pay a smaller dividend than ϕq . Moreover, because leveraged ETFs often have other sources of income, e.g. interest income from the proceeds of short sales, understanding dividend dynamics needs to be done on a case-by-case basis. We do note that it is also possible to infer an implied LETF dividend yield in the usual manner using put-call parity. For the purpose of this paper, however, we will assume a dividend yield of $\phi q + f$ as implied by (8) and simply note that it would be straightforward to handle other dividend assumptions.

⁴Because λ is a constant in our examples c_t is in fact a constant. We could, however, also use our approach for more general point processes such as affine processes which are also tractable.

The Path Dependence of Leveraged ETF Prices

While clear from (2) in the case of a diffusion, it is worth emphasizing that the risk-neutral dynamics of (8) yield a terminal value of L_T that is path-dependent. In particular L_T cannot be expressed as a function of S_T and so pricing an option on L_T does not amount to simply pricing some derivative of S_T .

3 Heston's Stochastic Volatility Model

The first model that we consider is Heston's[14] stochastic volatility (SV) model and we will see that it is particularly easy to price LETF options under this model. We assume the underlying ETF price, S_t , has risk-neutral dynamics given by

$$\frac{dS_t}{S_t} = (r - q)dt + \sqrt{V_t}dW_t^S, \quad (10)$$

$$dV_t = \kappa(\theta - V_t)dt + \gamma\sqrt{V_t}dW_t^V \quad (11)$$

where q is the dividend yield and W_t^S and W_t^V are standard Brownian motions with constant correlation parameter, ρ . Our first result is particularly straightforward and states that if S_t has Heston dynamics then so too does L_t .

Proposition 1. *Suppose the underlying ETF price S_t , has Heston dynamics given by (10) and (11). Then assuming a leverage ratio of ϕ , the LETF price, L_t , has dynamics given by*

$$\frac{dL_t}{L_t} = (r - q_L)dt + \text{sign}(\phi) \cdot \sqrt{V_t^L}dW_t^S \quad (12)$$

$$dV_t^L = \kappa_L(\theta_L - V_t^L)dt + \gamma_L\sqrt{V_t^L}dW_t^V \quad (13)$$

where $V_t^L := \phi^2 V_t$, $q_L := \phi q + f$, $\kappa_L := \kappa$, $\gamma_L := |\phi|\gamma$ and $\theta_L := \phi^2 \theta$. In particular the LETF also has Heston dynamics.

Proof : Since S_t follows a diffusion we note that (1) and (3) are identical. If we therefore substitute (10) into (3) we obtain $dL_t/L_t = (r - \phi q)dt + \phi\sqrt{V_t}dW_t^S$ which immediately yields (12). Similarly, using (11) we obtain $dV_t^L = \phi^2\kappa(\theta - V_t)dt + \phi^2\gamma\sqrt{V_t}dW_t^V$ which yields (13). ■

Proposition 1 shows that if S_t has Heston dynamics with parameter set $(q, \kappa, \gamma, \theta, V_0, \rho)$ then L_t has Heston dynamics with parameter set

$$(q_L, \kappa_L, \gamma_L, \theta_L, V_0^L, \rho_L) := (\phi q + f, \kappa, |\phi|\gamma, \phi^2 \theta, \phi^2 V_0, \text{sign}(\phi) \cdot \rho). \quad (14)$$

Since it is easy to price options using transform methods under the Heston model, Proposition 1 implies that we can price options on ETFs and LETFs consistently with each other when the ETF has Heston dynamics. While this result was very easy to derive we have not seen it elsewhere in the literature. In his PhD thesis, for example, Zhang [17] considers the pricing of LETF options when the underlying has Heston dynamics. He does not observe that L_t also has Heston dynamics, however, probably because he worked with (2) rather than (1). Indeed Zhang proposed a change

of measure motivated by (2) and observed that L_t had Heston dynamics with time-dependent parameters under this new measure. The time-dependency of the parameters under the new measure does not allow options on the LETF to be calculated via transform methods, however.

One further remark is in order at this point. It should be clear that the tractability that the LETF dynamics inherits from the underlying price dynamics will hold for diffusions in general and not just the Heston model. This should be clear from (1).

4 The SVJ Model

The Bates [4] stochastic volatility (SVJ) model is an extension of the SV model that allows for the possibility of jumps in the security price process. The risk-neutral dynamics for the SVJ model are

$$\frac{dS_t}{S_{t-}} = (r - q - \lambda m)dt + \sqrt{V_t}dW_t^S + dJ_t, \quad (15)$$

$$dV_t = \kappa(\theta - V_t)dt + \gamma\sqrt{V_t}dW_t^V \quad (16)$$

where W_t^S and W_t^V are standard Brownian motions with correlation coefficient ρ , N_t is a Poisson process with intensity λ , and $J_t := \sum_{i=1}^{N_t} (Y_i - 1)$ so that $Y_i - 1$ represents the relative jump size in the security price at the time of the i^{th} jump. In particular, if the i th jump occurs at time τ_i , then $S_{\tau_i} = S_{\tau_i-}Y_i$. The Y_i 's are assumed to be IID log-normally distributed with $\log Y_i \sim N(a, b^2)$ with $m := \mathbb{E}(Y_i - 1) = \exp\left(a + \frac{b^2}{2}\right) - 1$.

Proposition 2. *If S_t has risk-neutral dynamics given by (15) and (16) then the risk-neutral dynamics of L_t satisfy*

$$\frac{dL_t}{L_{t-}} = (r - q_L - \lambda m_L)dt + \text{sign}(\phi)\sqrt{V_t^L}dW_t^S + dJ_t^L \quad (17)$$

$$dV_t^L = \kappa_L(\theta_L - V_t^L)dt + \gamma_L\sqrt{V_t^L}dW_t^V \quad (18)$$

where $V_t^L := \phi^2 V_t$, $q_L := \phi q + f$, $\kappa_L := \kappa$, $\gamma_L := |\phi|\gamma$, $\theta_L := \phi^2\theta$, and $J_t^L := \sum_{i=1}^{N_t} (Y_i^L - 1)$ where

$$\begin{aligned} Y_i^L &:= \max(\phi(Y_i - 1), -1) + 1 \\ m_L &:= (1 - p^*) \cdot \mathbb{E}^Q[\phi(Y_i - 1) | \phi(Y_i - 1) > -1] - p^* \\ \text{and } p^* &:= Q(\phi(Y_i - 1) < -1) = \begin{cases} F\left(\log\left(\frac{\phi-1}{\phi}\right); a, b\right), & \text{if } \phi > 0 \\ 1 - F\left(\log\left(\frac{\phi-1}{\phi}\right); a, b\right), & \text{if } \phi < 0 \end{cases} \end{aligned} \quad (19)$$

where $F(\cdot; a, b)$ is the CDF of the $N(a, b)$ distribution.

Proof : (17) follows from (8). Since $V_t^L := \phi^2 V_t$ it is also clear that (18) follows directly from (16). ■

We would like to price options on the LETF using standard transform methods based on calculating the characteristic function of the log-LETF price. But first, we will distinguish between two types of jumps. We say that a jump, Y , is of type I if it satisfies $\max(\phi(Y - 1) + 1, 0) = 0$. Such a

jump would drive L_t to zero. Otherwise, it is of type II. A jump is type I with probability p^* and type II with probability $1 - p^*$ where p^* is defined in (19). Let $N_1(t)$ and $N_2(t)$ denote respectively the number of type I and type II jumps occurring in $[0, t]$. By the thinning property of Poisson processes, $N(t) = N_1(t) + N_2(t)$ where $N_1(t)$ and $N_2(t)$ are independent Poisson processes with rates λp^* and $\lambda(1 - p^*)$, respectively. We then have the following proposition.

Proposition 3. *Let $C(L_0, K, T)$ be the time $t = 0$ price of a call option on the LETF with strike K , maturity T and initial LETF price, L_0 . Then $C(L_0, K, T) = \exp(-\lambda p^* T) \hat{C}(L_0, K, T)$ where*

$$\hat{C}(L_0, K, T) := \mathbb{E}_0^Q[e^{-rT}(L_T - K)^+ | N_1(T) = 0] \quad (20)$$

is the value of the option given that there are no type I jumps in $[0, T]$.

Proof: The proof is immediate once we note that a type I jump will cause the LETF price to immediately fall to zero so that the call option will expire worthless in that event. ■

We will compute LETF call option prices⁵ in the SVJ model by computing $\hat{C}(L_0, K, T)$ and then using Proposition 3. We would like to compute $\hat{C}(L_0, K, T)$ using numerical transform inversion methods⁶ applied to the characteristic function of the log-LETF price, L_t , conditional on $N_1(T) = 0$. Since the diffusion component of the LETF dynamics is Heston (and therefore easy to handle), the only difficulty is in computing the characteristic function of the jump component of the log-LETF price conditional on $N_1(T) = 0$.

Towards this end, let $\Phi_{J_2^L(T)}$ denote the characteristic function of the jump component of the log-LETF price conditional on $N_1(T) = 0$. Then a standard expression for the characteristic function of a compound Poisson process yields

$$\begin{aligned} \Phi_{J_2^L(T)}(u) &= \mathbb{E}_0^Q \left[\exp \left(iu \cdot \sum_{j=1}^{N(T)} \log(Y_j^L) \right) \middle| N_1(T) = 0 \right] \\ &= \mathbb{E}_0^Q \left[\exp \left(iu \cdot \sum_{j=1}^{N_2(T)} \log(Y_j^L) \right) \right] \\ &= \exp[\lambda(1 - p^*)T(\Phi_X(u) - 1)] \end{aligned} \quad (21)$$

where $\Phi_X(\cdot)$ is the characteristic function of X with

$$X := (\log(\phi(Y - 1) + 1) \mid \phi(Y - 1) + 1 > 0). \quad (22)$$

If we can calculate $\Phi_X(\cdot)$, then it is easy to see that the characteristic function of the log-LETF price conditional on $N_1(T) = 0$ is given by

$$\Phi_L^{N_1=0}(u) := \exp(-\lambda m_L iuT) \Phi_T^{SV}(u; r, q_L, \kappa_L, \gamma_L, \theta_L, V_0^L, \rho_L, L_0) \times \exp[\lambda(1 - p^*)T(\Phi_X(u) - 1)]. \quad (23)$$

⁵Put prices can then be obtained from put-call parity.

⁶We use the Carr-Madan [5] Fourier inversion approach throughout the paper.

We could then use (23) together with the Carr-Madan [5] approach to compute $\hat{C}(L_0, K, T)$ in (20) and therefore obtain our LETF call option prices. We cannot compute $\Phi_X(\cdot)$ analytically, however, and so we must compute it numerically. Since the density function of X is known⁷, we can compute $\Phi_X(u)$ for a given u via numerical integration. Our approach then is to pre-calculate $\Phi_X(u)$ on a fine grid $u = u_1, \dots, u_N$ and then for an arbitrary u , we will approximate $\Phi_X(u)$ with $\Phi_X(u_j)$ where u_j is the closest grid-point to u . Using a suitably fine grid we can obtain a very good approximation to $\Phi_X(\cdot)$ which in turn yields a very accurate approximation, $\hat{\Phi}_L^{N_1 \equiv 0}(\cdot)$, that we can use in place of (23).

5 The SVCJ Model

The stochastic volatility model (SVCJ) with contemporaneous jumps in price and variance was introduced by Duffie, Pan and Singleton [7]. The risk-neutral dynamics for this model are

$$\frac{dS_t}{S_{t-}} = (r - q - \lambda m)dt + \sqrt{V_t}dW_t^S + dJ_t^S, \quad (24)$$

$$dV_t = \kappa(\theta - V_t)dt + \gamma\sqrt{V_t}dW_t^V + dJ_t^V \quad (25)$$

where $J_t^S := \sum_{i=1}^{N_t}(Y_i - 1)$, $J_t^V := \sum_{i=1}^{N_t} Z_i$ and N_t is a Poisson process with intensity λ . As before $Y_i - 1$ represents the percentage change in the security price due to the i th jump size and Z_i is the corresponding change in variance. In particular if the i th jumps occur at time τ_i , then $S_{\tau_i} = S_{\tau_i-}Y_i$ and $V_{\tau_i} = V_{\tau_i-} + Z_i$. We also assume the jumps in security price and variance are correlated. More precisely, we assume the Z_i 's are exponentially distributed with mean, μ_v , and that conditional on Z_i , $\log(Y_i)$, is normally distributed with mean, $a + \rho_J Z_i$, and variance, b^2 . In other words,

$$Z_i \sim \text{Exp}(\mu_v^{-1}) \quad (26)$$

and

$$\log(Y_i) \sim N(a, b^2) + \rho_J Z_i \sim N(a, b^2) + \text{sign}(\rho_J) \cdot \text{Exp}(c) \quad (27)$$

where $c := |\rho_J \mu_v|^{-1}$ and the normal and exponential components in (27) are independent. We also have $\text{Corr}(Z_i, \log(Y_i)) = \text{sign}(\rho_J) \cdot ((bc)^2 + 1)^{-1/2}$ which approaches ± 1 as b goes to 0 and see that $m = \mathbb{E}(Y_i - 1) = \exp(a + b^2/2) c / (c - \text{sign}(\rho_J)) - 1$. Finally note that W_t^S and W_t^V are standard Brownian motions with constant correlation coefficient, ρ . We have the following proposition describing the risk-neutral dynamics of L_t in the SVCJ model.

Proposition 4. *If S_t has risk-neutral dynamics given by (24) and (25) then the LETF with leverage ratio ϕ has risk-neutral dynamics*

$$\frac{dL_t}{L_{t-}} = (r - q_L - \lambda m_L)dt + \text{sign}(\phi)\sqrt{V_t^L}dW_t^S + dJ_t^L \quad (28)$$

$$dV_t^L = \kappa_L(\theta_L - V_t^L)dt + \gamma_L\sqrt{V_t^L}dW_t^V + d(\phi^2 J_t^V) \quad (29)$$

⁷We can define X as $X := [g(\log(Y_i)) \mid \phi(Y_i - 1) + 1 > 0]$ where $g(x) := \log(\phi(e^x - 1) + 1)$. Letting $f(\cdot; a, b)$ denote the density of $\log(Y) \sim N(a, b)$, we obtain

$$q(x) = \frac{f(g^{-1}(x); a, b)}{\mathbb{P}(\phi(Y_i - 1) + 1 > 0)} \cdot \left| \frac{d}{dx}(g^{-1}(x)) \right| = \frac{\text{sign}(\phi)}{1 - p^*} \cdot f\left(\log\left(\frac{e^x + \phi - 1}{\phi}\right); a, b\right) \cdot \frac{e^x}{e^x + \phi - 1}$$

as the density of X .

where $V_t^L := \phi^2 V_t$, $q_L := \phi q + f$, $\kappa_L := \kappa$, $\gamma_L := |\phi|\gamma$, $\theta_L := \phi^2 \theta$, $J_t^L := \sum_{i=1}^{N_t} (Y_i^L - 1)$ and

$$\begin{aligned} Y_i^L &:= \max(\phi(Y_i - 1), -1) + 1 \\ p^* &:= Q(\phi(Y_i - 1) < -1) = \begin{cases} P\left(\log(Y_i) < \log\left(\frac{\phi-1}{\phi}\right)\right), & \text{if } \phi > 0 \\ P\left(\log(Y_i) > \log\left(\frac{\phi-1}{\phi}\right)\right), & \text{if } \phi < 0 \end{cases} \\ \text{and } m_L &:= (1 - p^*) \cdot \mathbb{E}^Q[\phi(Y - 1) | \phi(Y - 1) > -1] - p^*. \end{aligned} \quad (30)$$

Proof : (28) follows directly from (8) and since $V_t^L := \phi^2 V_t$, (29) follows immediately from (25). ■

The question that now arises is whether or not we can price options on the LETF with dynamics given by (28) and (29). We could try to use the approach we adopted for the SVJ model where we pre-computed $\Phi_X(\cdot)$ on a fine grid of points but this does not seem like a very promising approach for two reasons. First, X will be a bivariate random variable under the SVCJ model (see (31) below) and so we would need to pre-compute $\Phi_X(\cdot)$ on a two-dimensional grid. Second, and more importantly, under the SVCJ model the characteristic function of the log-LETF price must be computed as the solution of a series of ODEs (see Appendix B.3) which depend in part on $\Phi_X(\cdot)$. Because this characteristic function is then used as an input to price LETF options via numerical transform inversion it is desirable to have an analytic expression for it. Unfortunately we do not have an analytic expression for $\Phi_X(\cdot)$ under the SVCJ model.

We will therefore proceed by approximating the dynamics of the LETF with more tractable dynamics. But first note that if we define Type I and Type II jumps as before then Proposition 3 remains valid under the SVCJ model so that (20) still holds, i.e. $C(L_0, K, T) = \exp(-\lambda p^* T) \hat{C}(L_0, K, T)$ where $\hat{C}(L_0, K, T) := \mathbb{E}_0^Q[e^{-rT}(L_T - K)^+ | N_1(T) = 0]$ is the value of the option given that there are no type I jumps in $[0, T]$. Our goal will be to approximate the option price by approximating $\hat{C}(L_0, K, T)$. To do this we let

$$\begin{aligned} X &:= (X_1, X_2) \\ &:= ((\log(\phi(Y_i - 1) + 1), \phi^2 Z_i) \mid \phi(Y_i - 1) + 1 > 0) \\ &= ((\log(Y_i^L), \phi^2 Z_i) \mid \phi(Y_i - 1) + 1 > 0) \end{aligned} \quad (31)$$

be the bivariate random vector representing jumps in the log-LETF price and its variance process, respectively. As stated above, we would like to have a closed-form expression for the characteristic function, $\Phi_X(\cdot)$, of X so that we could then apply the methodology of Duffie et al. [7] to compute the characteristic function of the log-LETF price.

We don't have such a closed form expression, however, so we will instead approximate X with another bivariate distribution whose characteristic function is available in closed-form. In particular, we will approximate X with a combination of univariate normal and bivariate exponential (BVE) distributions where the parameters of the approximating distribution will be chosen via a simple moment-matching procedure. Moment-matching is a standard approximation approach and it has been employed successfully in many domains including (see for example Glasserman and Merener [11]) the pricing of financial derivatives. The specific details of the moment-matching algorithm are provided in Appendix B.2. As with many approximation approaches, it is necessary to tailor the approach to the problem at hand. In this case we have chosen the normal-BVE

distribution to approximate X as defined for the SVCJ model as we have found⁸ it to be capable of providing a very good fit in this case. For other affine jump-diffusion models the normal-BVE distribution may not be suitable and so it would be necessary⁹ to use some other suitably tractable distribution.

6 Model Calibration

We considered three different parameter sets for our numerical experiments. The first set was obtained by calibrating each of the models to 6-month call options on the underlying security in a low volatility environment. The call option strikes ranged from \$60 to \$140. The low volatility regime was characterized by a relatively flat skew and an at-the-money (ATM) volatility of approximately 20%. The second parameter set was obtained by calibrating the three models to 6-month call options on the underlying security in a high volatility environment with a steeper skew and an ATM volatility of approximately 72%. This high volatility environment was typical of the environment that prevailed at the height of the financial crisis of 2008. The third parameter set was obtained by calibrating each of the models to 1-month call option prices in the same high volatility environment that we used for the second parameter set. These environments can be seen in Figure 1 where we also assumed the underlying price, S_0 , was \$100. To be clear, the three environments were not obtained from any real market data and therefore constitute an artificially created data-set. Nonetheless it is clear from Figure 1 that these environments are representative of what might be seen in practice.

In each of our models we assumed $r = 0.01$ and $q = f = 0$. With the exception of ρ , the remaining model parameters in each model were calibrated by minimizing the sum-of-squares between the Black-Scholes implied volatilities in the given environment and the Black-Scholes volatilities implied by the model. The parameter ρ was fixed in advance as is commonly the case when calibrating Heston-style models. The reason for this is that it is well known that the sum-of-squares objective function tends to have so-called “valleys” or directions along which the objective function changes very little. This tends to create a problem for optimization routines and for this reason it is common to fix ρ in advance to some sensible value.

The Heston Model: We set $\rho = -0.7571$. The remaining parameters, $(\kappa, \gamma, V_0 = \theta)$, were obtained by minimizing the sum-of-squares as described above.

The SVJ Model: We set $\rho = -0.7571$ and then solved for the remaining six parameters, $(\kappa, \gamma, V_0 = \theta, \lambda, m, b)$.

The SVCJ Model: We set $\rho = -0.82$ and then solved for the remaining eight parameters, $(\kappa, \gamma, V_0 = \theta, \lambda, m, b, \mu_v, \rho_J)$.

Table 1 displays the calibrated parameters for each of the models in the three environments while Figure 1 shows that all three models were calibrated successfully to the given implied volatilities

⁸This observation is based on results from an earlier version of this paper where we fitted the normal-BVE distribution using a more complex optimization procedure. In this version of the paper we are using a simple moment-matching approach to fit the distribution. While the numerical results aren’t quite as good, moment-matching is easy to describe and a commonly employed approximation scheme.

⁹In Section 8 we will propose the saddlepoint approximation approach of Glasserman and Kim [9] for pricing LETF options under general AJD dynamics. Even then it is clear from [9] that it would be necessary to tailor the details of the saddlepoint approximation to the specific model dynamics under consideration.

Table 1: Model Parameters

Parameter set I (Calibrated to 6-month option prices in the low volatility environment.)

Parameters	SV Model	SVJ Model	SVCJ Model
Risk free rate r	0.01	0.01	0.01
Speed of mean reversion κ	10.95	0.5012	0.6097
Volatility of variance γ	0.2528	0.0895	0.0776
Long run mean variance θ	0.0421	0.0353	0.0393
Initial variance V_0	0.0421	0.0353	0.0393
Correlation ρ	-0.7571	-0.7571	-0.82
Jump arrival rate λ	n/a	1.0808	0.1406
m	n/a	-0.01	-0.0128
b	n/a	0.0745	0.1152
μ_v	n/a	n/a	0.01
ρ_J	n/a	n/a	0.0013

Parameter set II (Calibrated to 6-month option prices in the high volatility environment.)

Parameters	SV Model	SVJ Model	SVCJ Model
Risk free rate r	0.01	0.01	0.01
Speed of mean reversion κ	4.9498	0.6500	0.6500
Volatility of variance γ	1.1478	0.7895	0.3377
Long run mean variance θ	0.5505	0.3969	0.4048
Initial variance V_0	0.5505	0.3969	0.4048
Correlation ρ	-0.7571	-0.7571	-0.82
Jump arrival rate λ	n/a	2.1895	0.4996
m	n/a	-0.0105	-0.2592
b	n/a	0.2719	0.4588
μ_v	n/a	n/a	0.094
ρ_J	n/a	n/a	-0.2713

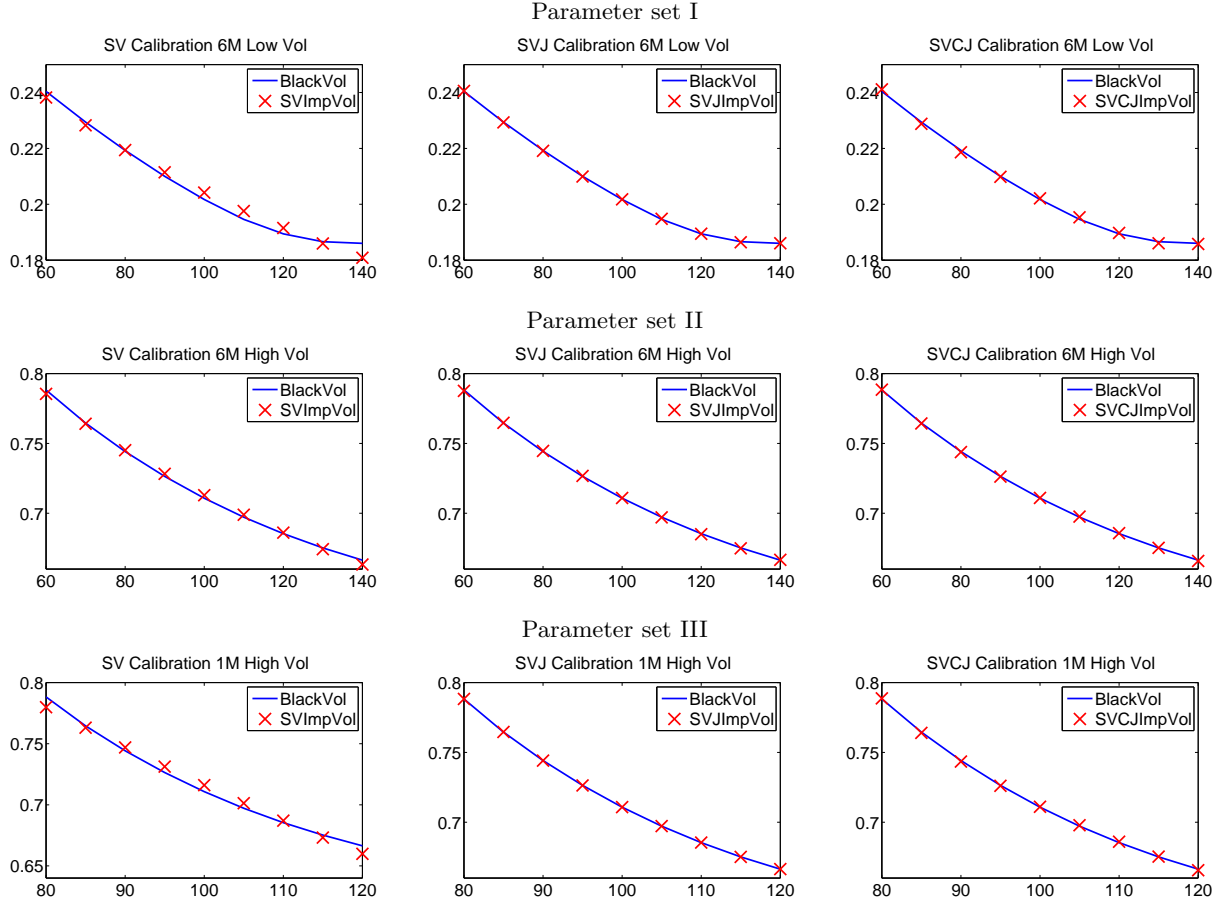
Parameter set III (Calibrated to 1-month option prices in the high volatility environment.)

Parameters	SV Model	SVJ Model	SVCJ Model
Risk free rate r	0.01	0.01	0.01
Speed of mean reversion κ	10.95	0.3632	0.5474
Volatility of variance γ	1.5086	0.6113	0.5730
Long run mean variance θ	0.5295	0.4156	0.4521
Initial variance V_0	0.5295	0.4156	0.4521
Correlation ρ	-0.7571	-0.7571	-0.82
Jump arrival rate λ	n/a	1.7483	0.5623
m	n/a	-0.1286	-0.2635
b	n/a	0.2384	0.3148
μ_v	n/a	n/a	0.0371
ρ_J	n/a	n/a	0.01

in each of the three environments. (The SV model doesn't calibrate quite as well but this is to be expected given that it has fewer parameters than the SVJ and SVCJ models.)

It is worth mentioning that we calibrated these models only to the prices of options written on the underlying index. An alternative and equally valid (though more difficult) approach would be to

Figure 1: Volatility skews for the underlying ETF



try and calibrate simultaneously to index *and* LETF option prices. We chose the former approach for several reasons. First, options on the underlying ETF are more liquid than the corresponding LETF option prices, and so it made sense to focus our calibration effort on these prices. Second, one of the questions we are interested in addressing in this paper is how LETF option prices varied across models. It was much easier to approach this problem by calibrating all models to index options prices only. If the goal is to treat options on the underlying index and LETF equally then it may be preferable to calibrate to both option types. This would certainly be possible but given the difficulty of pricing LETF options it would be considerably more time-consuming.

7 Numerical Results

In this section we compute LETF options prices by applying the Carr-Madan transform approach to the characteristic function of the log-LETF price (or approximate log-LETF price in the case of the SVCJ model). We will compare these approximate prices with exact prices obtained via Monte-Carlo. The advantage of the transform approach is that it is much faster than Monte-Carlo simulation and allows for the consistent price calculation and risk-management of ETF and LETF

Table 2: Option prices on underlying index / ETF for parameter set II computed via Monte-Carlo and transform inversion approaches. Approximate 95% confidence intervals are reported in brackets.

Moneyneess	BS vol (%)	BS price	Option price (SV)		Option price (SVJ)		Option price (SVCJ)	
$\frac{K}{S_0}$	Σ_{BS}	C_{BS}	C_{sim}	C_{tran}	C_{sim}	C_{tran}	C_{sim}	C_{tran}
0.75	75.44	33.66	33.66	33.66	33.66	33.66	33.65	33.65
			[33.65, 33.66]	-	[33.65, 33.67]	-	[33.65, 33.66]	-
1	71.08	20.04	20.10	20.10	20.05	20.05	20.06	20.05
			[20.09, 20.11]	-	[20.04, 20.06]	-	[20.05, 20.06]	-
1.25	68.03	11.24	11.23	11.23	11.23	11.22	11.25	11.24
			[11.23, 11.24]	-	[11.22, 11.23]	-	[11.24, 11.25]	-

options in almost real time.

The Monte-Carlo prices were obtained using the scheme of Andersen [1] which was designed to simulate the Heston model accurately. In the case of the SVJ and SVCJ models, we simply adapted Andersen to account for the independent jump processes. We assumed a time increment of $\Delta = 0.001$ which, assuming 250 trading days per year, corresponds to an interval of a quarter-day. Within the Monte-Carlo we assumed the LETF was re-balanced every 4 periods which is equivalent to the daily re-balancing that is performed in practice. Our first task is to compute option prices on the underlying ETF using the transform approach of Carr-Madan and Andersen’s Monte-Carlo scheme. Note that options on the underlying can be priced exactly using the transform approach as the characteristic function of the log-ETF price is available in this case for all three models. The reason we compute option prices on the underlying ETF is simply to check that the two sets of prices agree modulo statistical error from the simulation, and numerical inversion error from the Carr-Madan scheme.

Tables 2 and 3 display these ETF option prices for our three models under parameter sets II and III respectively. (All of our results for parameter set I, which corresponds to the low volatility 6-month environment, are deferred to Appendix C.) The Monte-Carlo results were based on simulating 10^8 sample paths which took¹⁰ several hours to run. We required this many paths to get sufficiently narrow confidence intervals so as to allow a comparison of the Monte-Carlo prices with the transform prices. It is clear from Tables 2 and 3 that both methods produce ETF option prices that effectively coincide with one another. Given this agreement we are now in a position to consider how well our pricing of LETF options actually performs, particularly¹¹ in the case of the SVJ and SVCJ models.

In Tables 4 and 5 we display prices of LETF options for parameter sets II and III, respectively, for each of our three models and various leverage ratios. (Recall that obtaining the Monte-Carlo prices took several hours so the discussion here refers only to the prices, C_{tran} , obtained via numerical transform inversion.) The most computationally demanding task was pricing the LETF options under the SVJ model: for each parameter set and each leverage ratio, it took about one minute

¹⁰All of our numerical experiments were implemented in **Matlab** version 7.12.0 (R2011a) on a Windows 7 machine with a 2.53 GHz processor and 4GB of RAM.

¹¹Recall that we needed to pre-compute numerically the characteristic function of the truncated jump component of the log-LETF price for the SVJ model, and that we needed to approximate its distribution for the SVCJ model.

Table 3: Option prices on underlying index / ETF for parameter set III computed via Monte-Carlo and transform inversion approaches. Approximate 95% confidence intervals are reported in brackets.

Moneyiness	BS vol(%)	BS price	Option price (SV)		Option price (SVJ)		Option price (SVCJ)	
$\frac{K}{S_0}$	Σ_{BS}	C_{BS}	C_{sim}	C_{tran}	C_{sim}	C_{tran}	C_{sim}	C_{tran}
0.9	74.42	13.98	14.01	14.01	13.98	13.98	13.97	13.98
			[14.01, 14.01]	-	[13.98, 13.99]	-	[13.97, 13.98]	-
1	71.08	8.04	8.10	8.10	8.05	8.04	8.05	8.05
			[8.10, 8.10]	-	[8.04, 8.05]	-	[8.04, 8.05]	-
1.1	68.54	4.09	4.10	4.10	4.09	4.09	4.10	4.10
			[4.10, 4.11]	-	[4.09, 4.09]	-	[4.09, 4.10]	-

to obtain the three option prices. Almost all of this time was spent computing the characteristic function of the log-truncated jump distribution on a grid of 10,000 points. Given the accuracy of the prices we obtained, we could easily have improved the run-time of these calculations by using a coarser grid of points. Moreover, we could have used instead the moment-matching approach that we adopted for the SVCJ model. While not quite as accurate, this latter approach only took approximately one tenth of a second to perform the moment-matching for a given leverage ratio and then price the three options corresponding to that ratio. Pricing the LETF options for the SV model took even less time as no approximations were required.

Before analyzing the results, we first consider the possible sources of discrepancy between the reported Monte-Carlo prices and the prices obtained via numerical transform inversion. There are four such sources:

- (i) Our Monte-Carlo assumed that the leveraged ETFs were re-balanced at a daily frequency as is the case in practice. The transform approach, however, implicitly assumes that the re-balancing takes place continuously. We will see in Table 6 below that this is a principal source of the discrepancy between the Monte-Carlo prices and the approximate prices.
- (ii) Numerical transform inversion is also a source of error but we believe this error to be very small and on the order of at most 1 or 2 cents. This claim is justified in part by the results in Tables 2 and 3.
- (iii) Statistical error in the reported Monte-Carlo prices. We ensured this error was small by simulating sufficiently many paths so as to ensure that the approximate 95% confidence intervals were just 1 or 2 cents wide.
- (iv) The fourth source are the errors that arise from: (i) the numerical pre-computation of the characteristic function of the truncated jump component of the log-LETF price in the case of the SVJ model and (ii) our approximation of the jump size distribution in the case of the SVCJ model.

The main observation from Tables 4 and 5 is that the approximate LETF option prices as reported in the C_{tran} columns are very close to the reported Monte-Carlo prices. The most noticeable

Table 4: Comparing leveraged ETFs option prices with approximate prices in parameter set II. Approximate 95% confidence intervals are reported in brackets.

Leverage ratio	Moneyness		Option price (SV)		Option price (SVJ)		Option price (SVCJ)	
	ϕ	$\frac{K_S}{S_0}$ $\frac{K_L}{L_0}$	C_{sim}	C_{tran}	C_{sim}	C_{tran}	C_{sim}	C_{tran}
2	0.75	0.5	60.74	60.66	61.51	61.44	61.66	61.61
			[60.72, 60.76]	-	[61.49, 61.53]	-	[61.64, 61.68]	-
		1	37.87	37.78	38.43	38.37	38.50	38.48
	1.25	1.5	[37.86, 37.89]	-	[38.41, 38.45]	-	[38.48, 38.51]	-
			24.18	24.11	24.45	24.41	24.66	24.70
			[24.16, 24.19]	-	[24.43, 24.46]	-	[24.65, 24.68]	-
3	0.75	0.25	81.98	81.82	83.25	83.06	82.39	82.27
			[81.94, 82.01]	-	[83.21, 83.29]	-	[82.35, 82.43]	-
		1	53.09	52.77	54.07	53.87	52.93	52.81
	1.25	1.75	[53.05, 53.12]	-	[54.03, 54.11]	-	[52.90, 52.97]	-
			37.60	37.30	37.84	37.69	37.33	37.29
			[37.57, 37.63]	-	[37.80, 37.87]	-	[37.30, 37.36]	-
-1	0.75	1.25	14.15	14.14	13.93	13.90	12.63	13.03
			[14.14, 14.16]	-	[13.92, 13.94]	-	[12.62, 12.64]	-
		1	21.19	21.15	21.16	21.10	20.00	20.36
	1.25	0.75	[21.18, 21.20]	-	[21.15, 21.17]	-	[19.99, 20.01]	-
			32.79	32.73	33.24	33.16	32.25	32.51
			[32.78, 32.80]	-	[33.23, 33.25]	-	[32.24, 32.26]	-
-2	0.75	1.5	32.09	31.88	31.29	31.01	27.94	27.94
			[32.05, 32.14]	-	[31.24, 31.33]	-	[27.91, 27.97]	-
		1	41.95	41.68	41.60	41.26	38.81	38.75
	1.25	0.5	[41.90, 41.99]	-	[41.56, 41.64]	-	[38.78, 38.84]	-
			60.25	60.02	61.09	60.76	59.08	59.01
			[60.21, 60.30]	-	[61.04, 61.13]	-	[59.05, 59.11]	-
-3	0.75	1.75	51.48	50.72	49.43	48.46	44.41	43.96
			[51.19, 51.77]	-	[49.18, 49.69]	-	[44.31, 44.51]	-
		1	60.88	60.17	59.56	58.59	55.77	55.30
	1.25	0.25	[60.59, 61.18]	-	[59.31, 59.82]	-	[55.67, 55.87]	-
			81.74	81.46	82.59	81.89	80.65	80.44
			[81.45, 82.04]	-	[82.33, 82.85]	-	[80.55, 80.76]	-

Table 5: Comparing leveraged ETFs option prices with approximate prices in parameter set III. Approximate 95% confidence intervals are reported in brackets.

Leverage ratio	Moneyness		Option price (SV)		Option price (SVJ)		Option price (SVCJ)	
ϕ	$\frac{K_S}{S_0}$	$\frac{K_L}{L_0}$	C_{sim}	C_{tran}	C_{sim}	C_{tran}	C_{sim}	C_{tran}
2	0.9	0.8	27.10	27.03	27.32	27.28	27.18	27.13
			[27.10, 27.11]	-	[27.32, 27.33]	-	[27.17, 27.19]	-
	1	1	15.98	15.94	16.06	16.04	15.97	15.94
			[15.98, 15.99]	-	[16.05, 16.06]	-	[15.96, 15.97]	-
	1.1	1.2	8.66	8.66	8.75	8.76	8.71	8.72
			[8.66, 8.67]	-	[8.74, 8.75]	-	[8.70, 8.71]	-
3	0.9	0.7	39.31	39.09	39.70	39.56	39.22	39.08
			[39.30, 39.32]	-	[39.69, 39.71]	-	[39.21, 39.23]	-
	1	1	23.65	23.49	23.78	23.70	23.45	23.38
			[23.65, 23.66]	-	[23.77, 23.79]	-	[23.44, 23.46]	-
	1.1	1.3	13.64	13.58	13.74	13.76	13.56	13.59
			[13.63, 13.65]	-	[13.74, 13.75]	-	[13.56, 13.57]	-
-1	0.9	1.1	4.81	4.84	4.54	4.55	4.57	4.51
			[4.81, 4.81]	-	[4.53, 4.54]	-	[4.57, 4.58]	-
	1	1	8.25	8.24	8.02	8.00	8.05	7.97
			[8.25, 8.25]	-	[8.02, 8.02]	-	[8.05, 8.06]	-
	1.1	0.9	13.58	13.53	13.48	13.44	13.50	13.40
			[13.57, 13.58]	-	[13.48, 13.49]	-	[13.49, 13.50]	-
-2	0.9	1.2	10.39	10.41	9.61	9.61	9.72	9.75
			[10.39, 10.40]	-	[9.60, 9.61]	-	[9.72, 9.73]	-
	1	1	16.58	16.49	15.96	15.86	16.06	15.98
			[16.58, 16.59]	-	[15.95, 15.97]	-	[16.05, 16.06]	-
	1.1	0.8	26.49	26.32	26.24	26.07	26.26	26.11
			[26.48, 26.50]	-	[26.23, 26.25]	-	[26.26, 26.27]	-
-3	0.9	1.3	16.72	16.61	15.19	15.11	15.44	15.33
			[16.71, 16.73]	-	[15.18, 15.20]	-	[15.43, 15.45]	-
	1	1	25.02	24.70	23.81	23.54	24.02	23.72
			[25.00, 25.03]	-	[23.80, 23.82]	-	[24.01, 24.03]	-
	1.1	0.7	38.74	38.31	38.23	37.87	38.31	37.91
			[38.73, 38.76]	-	[38.22, 38.25]	-	[38.30, 38.32]	-

discrepancy occurs for some options with leverage ratios of -3 in Table 4 where the discrepancy between the simulation and transform-based prices is sometimes on the order of 1% or 2%. But in a high volatility environment these errors should easily fall within the bid-ask spreads found in practice. We note that the errors are much smaller for the 3-month high-volatility environment options of Table 5 and are practically non-existent for the low-volatility environment of Table 15.

We also note that the Monte-Carlo prices are generally higher than the transform-based prices. This is presumably due to the fact that prices computed via the transform approach are based on continuous re-balancing of the LETFs whereas the Monte-Carlo prices are computed assuming the LETF is re-balanced daily. This is also suggested by the prices in the SV model where LETF option pricing is exact (modulo transform inversion error) but where we still see a discrepancy between Monte Carlo and transform prices that is comparable to the discrepancies we observe in the SVJ and SVCJ models.

We can confirm this observation by examining the option prices in Table 6 where we also report Monte-Carlo prices that were estimated assuming the LETF was re-balanced 4 times per day rather than just once per day. In that table we see that the Monte-Carlo prices based on re-balancing four times per day are generally much closer to the transform based prices. Presumably if we were to increase the LETF re-balancing frequency then the Monte-Carlo and transform-based prices would be in even closer agreement. These observations justify our earlier observation that most of the discrepancy in Tables 4 and 5 between the Monte-Carlo prices and transform-based prices is due to the differences in re-balancing frequency.

Another observation regarding Table 6 is that, with the exception of the SVCJ model, LETF option prices appear to be monotonic with respect to rebalancing frequency for a given leverage ratio and moneyness value. In particular, we see that $C_{sim}^{(1)} \geq C_{sim}^{(4)} \geq C_{tran}$ is generally satisfied for the SV and SVJ models. (Recall our earlier observation that C_{tran} corresponds to a continuous rebalancing assumption.) In the case of the SVCJ model we do observe that $C_{sim}^{(1)} \geq C_{sim}^{(4)}$ but the pattern is broken with C_{tran} . This is likely due to the fact that C_{tran} is computed using approximate LETF dynamics whereas the Monte-Carlo prices are computed using the true LETF dynamics.

A final observation from Tables 4 and 5 is that there is some discrepancy in LETF option prices across the three different models. For example, in Table 4 we see that with $\phi = -3$ and $K_L/L_0 = 1.75$ the LETF call option price is approximately \$51, \$49 and \$44 under the SV, SVJ and SVCJ models, respectively. This is despite the fact that all three models were calibrated to the same 6-month implied volatilities. Of course, this observation is not too surprising as the LETF price is path-dependent and so it is not the case that the 6-month LETF option prices will only depend on the risk-neutral distribution of S_t where $t = 6$ months. This difference in LETF option prices across models is less noticeable in the 1-month options of parameter set III in Table 5. It is also worth pointing out that the 6-month LETF option prices vary very little by model in the low-volatility environment of parameter set I. These prices are displayed in Appendix C. We will return to this issue in Section 7.1.

7.1 Comparing the LETF Implied Volatilities Across Different Models

We now report the LETF option prices in terms of their Black-Scholes implied volatilities. We have already seen that there is some variability in these prices across the different models but it

Table 6: Comparison of LETF option prices obtained by Monte-Carlo simulation with different re-balancing frequencies in parameter set II. $C_{sim}^{(1)}$ corresponds to daily re-balancing and $C_{sim}^{(4)}$ corresponds to re-balancing 4 times per day. C_{tran} refers to prices that were obtained via numerical transform inversion.

Leverage ratio	Moneyness		Option price (SV)			Option price (SVJ)			Option price (SVCJ)		
ϕ	$\frac{K_S}{S_0}$	$\frac{K_L}{L_0}$	$C_{sim}^{(1)}$	$C_{sim}^{(4)}$	C_{tran}	$C_{sim}^{(1)}$	$C_{sim}^{(4)}$	C_{tran}	$C_{sim}^{(1)}$	$C_{sim}^{(4)}$	C_{tran}
2	0.75	0.5	60.74	60.69	60.66	61.51	61.46	61.44	61.66	61.61	61.61
	1	1	37.87	37.81	37.78	38.43	38.39	38.37	38.50	38.46	38.48
	1.25	1.5	24.18	24.13	24.11	24.45	24.42	24.41	24.66	24.65	24.70
3	0.75	0.25	81.98	81.88	81.82	83.25	83.12	83.06	82.39	82.28	82.27
	1	1	53.09	52.87	52.77	54.07	53.92	53.87	52.93	52.80	52.81
	1.25	1.75	37.60	37.39	37.30	37.84	37.73	37.69	37.33	37.24	37.29
-1	0.75	1.25	14.15	14.14	14.14	13.93	13.90	13.90	12.63	12.62	13.03
	1	1	21.19	21.16	21.15	21.16	21.12	21.10	20.00	19.97	20.36
	1.25	0.75	32.79	32.74	32.73	33.24	33.18	33.16	32.25	32.21	32.51
-2	0.75	1.5	32.09	31.93	31.88	31.29	31.06	31.01	27.94	27.81	27.94
	1	1	41.95	41.74	41.68	41.60	41.33	41.26	38.81	38.65	38.75
	1.25	0.5	60.25	60.08	60.02	61.09	60.83	60.76	59.08	58.95	59.01
-3	0.75	1.75	51.48	50.80	50.72	49.43	48.59	48.46	44.41	43.99	43.96
	1	1	60.88	60.24	60.17	59.56	58.72	58.59	55.77	55.36	55.30
	1.25	0.25	81.74	81.43	81.46	82.59	81.96	81.89	80.65	80.48	80.44

would be interesting to see this variability expressed in units of implied volatility. This will also allow us to consider the commonly used practice of computing an LETF option price via the Black-Scholes formula with the implied volatility taken (and scaled appropriately) from a corresponding underlying index (or ETF) option price. We will also introduce an additional model, namely the Barndorff-Nielsen and Shephard (BNS) model (see [3]), as this model helps to provide an even clearer demonstration of the fact that LETF option prices are strongly path dependent and are not uniquely determined by the implied volatility surface of the underlying index or ETF. We first describe the BNS model.

The BNS Model: The variance process is modeled by an Ornstein-Uhlenbeck process driven by a Levy process with non-negative increments. In particular we will assume that the variance process is a Gamma-OU process and that the risk-neutral dynamics for the security price and instantaneous variance are

$$\begin{aligned}
d \log S_t &= \left(r - q - \frac{a\lambda\rho}{b-\rho} - \frac{V_t}{2} \right) dt + \sqrt{V_t} dW_t + \rho dz_{\lambda,t} \\
dV_t &= -\lambda V_t dt + dz_{\lambda,t}
\end{aligned}$$

where W_t is a standard Brownian motion and z_t is a compound Poisson process with $z_t = \sum_{n=1}^{N_t} x_n$ where the Poisson process, N_t , has intensity, a , and the x_i 's are IID exponential random variables with mean $1/b$. We also assume $\lambda > 0$ and $V_0 > 0$ so that (since $dz_{\lambda,t}$ is always non-negative) $\inf_{0 \leq t \leq T} V_t \geq \exp(-\lambda T) > 0$. The parameter, ρ , is typically negative to account for the negative correlation between variance and the underlying price process. Note that the variance can only jump upwards and that between jumps it decays exponentially. With a negative value of ρ the

Table 7: Comparison for the prices of options on the leveraged ETFs obtained by Monte-Carlo simulation in parameter sets II and III

Leverage ratio	Moneyness		Parameter Set II				Moneyness		Parameter Set III			
ϕ	$\frac{K_S}{S_0}$	$\frac{K_L}{L_0}$	C_{sim}^{SV}	C_{sim}^{SVJ}	C_{sim}^{SVCJ}	C_{sim}^{BNS}	$\frac{K_S}{S_0}$	$\frac{K_L}{L_0}$	C_{sim}^{SV}	C_{sim}^{SVJ}	C_{sim}^{SVCJ}	C_{sim}^{BNS}
2	0.75	0.5	60.74	61.51	61.66	63.20	0.9	0.8	27.10	27.32	27.18	27.50
	1	1	37.87	38.43	38.50	40.55	1	1	15.98	16.06	15.97	16.26
	1.25	1.5	24.18	24.45	24.66	26.64	1.1	1.2	8.66	8.75	8.71	8.93
3	0.75	0.25	81.98	83.25	82.39	85.18	0.9	0.7	39.31	39.70	39.22	40.50
	1	1	53.09	54.07	52.93	57.81	1	1	23.65	23.78	23.45	24.62
	1.25	1.75	37.60	37.84	37.33	42.29	1.1	1.3	13.64	13.74	13.56	14.47
-1	0.75	1.25	14.15	13.93	12.63	11.53	0.9	1.1	4.81	4.54	4.57	4.39
	1	1	21.19	21.16	20.00	18.92	1	1	8.25	8.02	8.05	7.86
	1.25	0.75	32.79	33.24	33.25	31.48	1.1	0.9	13.58	13.48	13.50	13.35
-2	0.75	1.5	32.09	31.29	27.94	24.88	0.9	1.2	10.39	9.61	9.72	9.18
	1	1	41.95	41.60	38.81	36.15	1	1	16.58	15.96	16.06	15.50
	1.25	0.5	60.25	61.09	59.08	57.72	1.1	0.8	26.49	26.24	26.26	25.88
-3	0.75	1.75	51.48	49.43	44.41	39.00	0.9	1.3	16.72	15.19	15.44	14.36
	1	1	60.88	59.56	55.77	51.48	1	1	25.02	23.81	24.02	22.97
	1.25	0.25	81.74	82.59	80.65	79.48	1.1	0.7	38.74	38.23	38.31	37.64

security price will jump downwards when a jump in variance occurs and it is worth noting in this case that leveraged ETFs with $\phi < 0$ can then only jump upwards in price. There is therefore no need to truncate the jumps of the LETF price process in this case and indeed the LETF price process will itself have BNS dynamics. When $\phi > 0$ this will not be true as it will be necessary to truncate the jumps of the underlying ETF. In this case we could try to approximate the jump-process as we did with the SVJ and SVCJ models and then obtain approximate LETF option prices using transform methods. Rather than doing this, however, we will simply price the LETF options using Monte-Carlo because our goal in this section is to simply investigate how model dependent LETF option prices are.

We calibrated the BNS model to the same implied volatility skews of Figure 1 and note here that this calibration was performed successfully so that all four models agreed on the prices of options on the underlying ETF. This agreement can be seen in Tables 10 and 11 by noting that the columns labeled Σ_S are practically identical across the four models. The prices of the LETF options across the four models and various leverage ratios are displayed in Table 7. The same results, except in terms of implied volatilities, are displayed in Tables 10 and 11 for parameter sets II and III, respectively. The LETF option implied volatilities are displayed in the columns labeled Σ_L and are calculated using the LETF option prices from Tables 4 and 5.

In order to compute the implied volatility ratios, $\frac{\Sigma_L}{\Sigma_S}$, we aligned the options on the underlying ETF and the leveraged ETF on a “strike-equivalent-basis” to account for the leverage. For example, we align a 25% OTM option on the underlying ETF with a 50% OTM option on a double-long LETF to account for the higher leverage of $\phi = 2$. We note that the implied volatility ratio tends to be

close to the leverage ratio, ϕ , but that there can be a considerable discrepancy between the two. The degree of this discrepancy is model dependent and is very notable for the BNS model (which is why we have included the BNS model here). For a given model, it is also the case that whether or not the ratio $\frac{\Sigma_L}{\Sigma_S}$ is greater than ϕ depends on whether or not the LETF is positively or negatively leveraged. We emphasize again here that these observations are based on parameter set II which models the 6-month, high volatility environment.

8 Saddlepoint Approximations

The affine-jump-diffusion (AJD) models of Duffie et al. [7] is a rich and flexible class under which the prices of many derivative security types can be obtained via the numerical inversion of extended transforms. In general, however, these extended transforms can only be computed numerically as the solution of a series of ODEs. In order to compute derivative security prices it is therefore necessary (in general) to solve a series of ODEs for each integration point in the aforementioned numerical transform inversion. This has limited application of AJD models in practice to the much smaller subset of models for which the transforms are available in closed form. We note that even though the SVJ and SVCJ models considered in this paper are AJD models where the transforms are known in closed form, this is not true for the LETF dynamics in those models: truncating the jumps results in AJD models where the transforms are not available in closed form.

Glasserman and Kim [10] proposed the use of saddlepoint approximations to tackle this issue. More specifically, it is well known that the calculation of option prices can be reduced to the calculation of tail probabilities of the form $Q(Y > y)$ where $Y = \log(S_T)$, the log-security price at time T , and Q is an equivalent martingale measure corresponding to some given numeraire. In the AJD setting this tail probability can be calculated via Fourier inversion according to

$$Q(Y > y) = \frac{1}{2\pi i} \int_{\tau-i\infty}^{\tau+i\infty} e^{(\mathcal{K}(z)-zy)} \frac{dz}{z}, \quad \tau > 0 \quad (32)$$

where \mathcal{K} is the cumulant-generating function (CGF) of the log-security price, i.e. $e^{\mathcal{K}(z)} = \mathbb{E}(e^{z \log(S_T)})$. We can therefore price options by performing a numerical integration to compute the right-hand-side of (32). Unfortunately, for each evaluation point, z , in the numerical integration, we must in general solve a series of ODEs to compute $\mathcal{K}(z)$. As mentioned above, this seriously limits the applicability of AJD models to those models where $\mathcal{K}(z)$ is available in closed form.

Glasserman and Kim's contribution was to recognize that if $\mathcal{K}(z)$ is not available in closed form, then it would still be possible to obtain an accurate approximation to (32) using a saddlepoint approximation. Their approximation requires the calculation of $\mathcal{K}(\hat{z})$ as well as the first and second derivatives, $\mathcal{K}'(\hat{z})$ and $\mathcal{K}''(\hat{z})$, at the saddlepoint, \hat{z} . The saddlepoint satisfies $\mathcal{K}'(\hat{z}) = y$ and most of the computational work is expended in solving¹² this equation. (Calculation of $\mathcal{K}(\hat{z})$, $\mathcal{K}'(\hat{z})$ and $\mathcal{K}''(\hat{z})$ requires solving three systems of ODEs. This is a significant improvement over having to solve a system of ODEs for each integration point, z .) In their numerical experiments, Glasserman and Kim obtain accurate option prices via their saddlepoint approximations but they also find that no

¹²Glasserman and Kim consider several approaches for finding \hat{z} including the Lieberman approximation, the Lugannani-Rice (LR) formula and variations of the LR formula.

Table 8: Comparing LETF option prices in the SV model under parameter set II. $C_{saddlepoint}$ refers to prices that were obtained via a saddlepoint approximation.

Leverage ratio	Moneyness		Option price			
	ϕ	$\frac{K_S}{S_0}$	$\frac{K_L}{L_0}$	C_{sim}	C_{tran}	$C_{saddlepoint}$
2		0.75	0.5	60.74	60.66	60.66
		1	1	37.87	37.78	37.78
		1.25	1.5	24.18	24.11	24.10
3		0.75	0.25	81.98	81.82	81.82
		1	1	53.09	52.77	52.76
		1.25	1.75	37.60	37.30	37.29
-1		0.75	1.25	14.15	14.14	14.14
		1	1	21.19	21.15	21.15
		1.25	0.75	32.79	32.73	32.72
-2		0.75	1.5	32.09	31.88	31.88
		1	1	41.95	41.68	41.67
		1.25	0.5	60.25	60.02	60.01
-3		0.75	1.75	51.48	50.72	50.72
		1	1	60.88	60.17	60.17
		1.25	0.25	81.74	81.46	81.46

one approach dominates. While their LR approximation provides the best overall performance they recommend¹³ tailoring the specific approximation to the level of moneyness and time-to-maturity.

In order to examine the performance of the saddlepoint technique for pricing LETF options, we applied¹⁴ it to the SV model under the high-volatility parameter sets II and III. In Tables 8 and 9 we compare the LETF option prices that were obtained using three different methods: Monte-Carlo, numerical transform inversion and saddlepoint approximation. (Recall that when the underlying index / ETF has SV dynamics, then the LETF also has SV dynamics and therefore numerical transform inversion yields exact option prices (assuming continuous re-balancing of the LETF).) We see that the transform inversion and saddlepoint prices practically coincide: the price difference is a cent or less in every case. This admittedly limited experiment suggests that the saddlepoint approach is also capable of producing accurate LETF option prices for other AJD price dynamics. Given the observations of Glasserman and Kim, however, it's unlikely that the saddlepoint approach can be used in a black-box fashion for all AJD models. In particular, some tailoring of the approach to each model under consideration would be required.

¹³In a similar spirit, we would recommend tailoring jump distribution of moment-matching approach to the specific AJD model under consideration.

¹⁴We are grateful to Kyoung-Kuk Kim for providing us with `Matlab` code that we could easily adapt to pricing the LETF options in the SV model.

Table 9: Comparing LETF option prices in the SV model under parameter set III. $C_{saddlepoint}$ refers to prices that were obtained via a saddlepoint approximation.

Leverage ratio ϕ	Moneyness		Option price		
	$\frac{K_S}{S_0}$	$\frac{K_L}{L_0}$	C_{sim}	C_{tran}	$C_{saddlepoint}$
2	0.9	0.8	27.10	27.03	27.03
	1	1	15.98	15.94	15.94
	1.1	1.2	8.66	8.66	8.66
3	0.9	0.7	39.31	39.09	39.09
	1	1	23.65	23.49	23.49
	1.1	1.3	13.64	13.58	13.59
-1	0.9	1.1	4.81	4.84	4.84
	1	1	8.25	8.24	8.24
	1.1	0.9	13.58	13.53	13.53
-2	0.9	1.2	10.39	10.41	10.41
	1	1	16.58	16.49	16.49
	1.1	0.8	26.49	26.32	26.32
-3	0.9	1.3	16.72	16.61	16.61
	1	1	25.02	24.70	24.70
	1.1	0.7	38.74	38.31	38.31

9 Conclusions

We have shown how to obtain accurate LETF option prices via transform pricing methods for the Heston (SV) model as well as two related jump-diffusion models, namely the SVJ and SVCJ models. Our option prices for the SV and SVJ models were exact but in the case of the SVCJ model we proposed approximate price dynamics for the LEFT based on approximating its (truncated) jump distribution. We find our methodology works very well in both low and high volatility environments and because they are consistent with the prices of options on the underlying ETF, they permit consistent pricing and risk-management of derivatives portfolios containing both ETF and LETF options. It should also be clear that similar approximation techniques could be applied to other jump-diffusion models and so our examples should be viewed as applications of a more general approximation technique. We have also proposed the saddlepoint approximation approach of Glasserman and Kim [9] as an alternative approach which can be used for general affine jump-diffusion price dynamics. Nevertheless, we note that these approximation methods do need to be tailored to the specific model under consideration.

In addition to confirming the accuracy of our LETF option prices, our numerical experiments also showed that the ratio of an LETF option implied volatility to the corresponding ETF option implied volatility can be far from the LETF leverage ratio. The difference between the two depends on whether or not the LETF is long or short and is model dependent, thereby emphasizing the path dependence of the LETF price at any given time. This calls into question the market practice of pricing an LETF option using the Black-Scholes formula with the strike and implied volatility from the underlying ETF scaled by the leverage ratio. In particular, it should be clear that using the

Black-Scholes formula in this manner amounts to the implicit assumption of (generally unspecified) dynamics for the underlying ETF.

Table 10: Comparison of Black-Scholes Implied-Volatilities: Parameter Set II

Leverage ratio	Moneyneess		Implied Volatility (SV)			Implied Volatility (SVJ)			Implied Volatility (SVCJ)			Implied Volatility (BNS)		
	$\frac{K_S}{S_0}$	$\frac{K_L}{L_0}$	Σ_S	Σ_L	$\frac{\Sigma_L}{\Sigma_S}$	Σ_S	Σ_L	$\frac{\Sigma_L}{\Sigma_S}$	Σ_S	Σ_L	$\frac{\Sigma_L}{\Sigma_S}$	Σ_S	Σ_L	$\frac{\Sigma_L}{\Sigma_S}$
ϕ														
2	0.75	0.5	75.42	149.10	1.98	75.44	154.61	2.05	75.40	155.73	2.07	75.41	166.68	2.21
	1	1	71.28	139.11	1.95	71.10	141.35	1.99	71.13	141.62	1.99	71.09	149.98	2.11
	1.25	1.5	68.00	133.12	1.96	67.98	134.07	1.97	68.05	134.85	1.98	68.04	141.88	2.09
3	0.75	0.25		224.18	2.97		242.31	3.21		230.05	3.05		270.14	3.58
	1	1		204.20	2.86		208.76	2.94		203.50	2.86		226.66	3.19
	1.25	1.75		195.88	2.88		196.76	2.89		194.89	2.86		213.52	3.14
-1	0.75	1.25		78.48	1.04		77.69	1.03		73.04	0.97		69.07	0.92
	1	1		75.29	1.06		75.20	1.06		70.93	1.00		66.95	0.94
	1.25	0.75		71.11	1.05		73.36	1.08		68.39	1.01		64.44	0.95
-2	0.75	1.5		161.47	2.14		158.55	2.10		146.52	1.94		135.62	1.80
	1	1		155.70	2.18		154.26	2.17		142.90	2.01		132.23	1.86
	1.25	0.5		145.60	2.14		151.60	2.23		137.08	2.01		126.99	1.87
-3	0.75	1.75		250.11	3.32		241.67	3.20		221.67	2.94		201.07	2.67
	1	1		242.04	3.40		235.34	3.31		216.79	3.05		196.86	2.77
	1.25	0.25		220.82	3.25		232.95	3.43		205.07	3.01		187.56	2.76

Table 11: Comparison of Black-Scholes Implied-Volatilities: Parameter Set III

Leverage ratio	ϕ	Moneyneess $\frac{K_S}{S_0}$	$\frac{K_L}{L_0}$	Implied Volatility (SV)			Implied Volatility (SVJ)			Implied Volatility (SVCJ)			Implied Volatility (BNS)		
				Σ_S	Σ_L	$\frac{\Sigma_L}{\Sigma_S}$	Σ_S	Σ_L	$\frac{\Sigma_L}{\Sigma_S}$	Σ_S	Σ_L	$\frac{\Sigma_L}{\Sigma_S}$	Σ_S	Σ_L	$\frac{\Sigma_L}{\Sigma_S}$
2		0.9	0.8	74.70	149.29	2.00	74.43	151.86	2.04	74.33	150.19	2.02	74.47	153.92	2.07
		1	1	71.59	142.28	1.99	71.09	142.98	2.01	71.10	142.18	2.00	71.09	144.82	2.04
		1.1	1.2	68.68	136.37	1.99	68.55	137.13	2.00	68.61	136.78	1.99	68.57	138.82	2.02
3		0.9	0.7		224.42	3.00		229.50	3.08		223.22	3.00		239.89	3.22
		1	1		212.51	2.97		213.65	3.01		210.62	2.96		221.45	3.12
		1.1	1.3		203.50	2.96		204.42	2.98		202.82	2.96		210.92	3.08
-1		0.9	1.1		75.38	1.01		72.78	0.98		73.14	0.98		71.41	0.96
		1	1		72.90	1.02		70.85	1.00		71.16	1.00		69.40	0.98
		1.1	0.9		70.06	1.02		69.04	1.01		69.18	1.01		67.55	0.99
-2		0.9	1.2		152.14	2.04		145.04	1.95		146.08	1.97		141.10	1.89
		1	1		147.73	2.06		142.09	2.00		142.95	2.01		137.94	1.94
		1.1	0.8		142.13	2.07		139.12	2.03		139.43	2.03		134.80	1.97
-3		0.9	1.3		231.00	3.09		217.39	2.92		219.57	2.95		209.93	2.82
		1	1		225.17	3.15		213.95	3.01		215.89	3.04		206.21	2.90
		1.1	0.7		216.96	3.16		210.24	3.07		211.25	3.08		202.31	2.95

References

- [1] L. Andersen. Efficient simulation of the heston stochastic volatility model, January 2007.
- [2] M. Avellaneda and S.J.Zhang. Path-dependence of leveraged etf returns. *SIAM Journal of Financial Mathematics*, 1:586–603, 2010.
- [3] O.E. Barndorff-Nielsen and N. Shephard. Non-gaussian ornstein-uhlenbeck-based models and some of their uses in financial economics. *Journal of the Royal Statistical Society: Series B*, 63(2), 2001.
- [4] D. Bates. Exchange rate processes implicit in deutsche mark options. *Review of Financial Studies*, 7:69–107, 1996.
- [5] P. Carr and D. Madan. Option valuation using the fast fourier transform. *Journal of Computational Finance*, 2:61–73, 1998.
- [6] M. Cheng and A. Madhavan. The dynamics of leveraged and inverse exchange traded funds. *Journal of Investment Management*, Winter 2009, 2009.
- [7] D. Duffie, J. Pan, and K. Singleton. Transform analysis and asset pricing for affine jump-diffusions. *Econometrica*, 68(6):1343–1376, 2000.
- [8] Chicago Board Options Exchange. Cboe 2010 market statistics, 2010.
- [9] P. Glasserman and K. Kim. Saddlepoint approximations for affine jump-diffusion models. *Journal of Economic Dynamics and Control*, 33:37–52, 2009.
- [10] P. Glasserman and K. Kim. Saddlepoint approximations for affine jump-diffusion models. *Journal of Economic Dynamics and Control*, 33(1):15–36, 2009.
- [11] P. Glasserman and N. Merener. Cap and swaption approximations in libor market models with jumps. *Journal of Computational Finance*, 7(1):1–36, 2003.
- [12] M.B. Haugh. A note on constant proportion trading strategies. *Operations Research Letters*, 39(3):172–179, 2011.
- [13] M.B. Haugh and A. Jain. The dual approach to portfolio evaluation: A comparison of the static, myopic and generalized buy-and-hold strategies. *Quantitative Finance*, 11(1):81–99, 2011.
- [14] S. Heston. A closed-form solution for options with stochastic volatility with applications to bond and currency options. *Review of Financial Studies*, 6:327–343, 1993.
- [15] T. Leung and R. Sircar. Implied volatility of leveraged etf options, October 2012.
- [16] A.W. Marshall and I. Olkin. A multivariate exponential distribution. *Journal of the American Statistical Association*, 62:30–44, 1967.
- [17] J. Zhang. *Path dependence properties of leveraged exchange-traded funds: compounding, volatility and option pricing*. PhD thesis, NYU, 2010.
- [18] J. Zhu. *Applications of Fourier Transform to Smile Modeling*. Springer, 2010.

A Log-Price Characteristic Functions

The Heston Model: The characteristic function of the log-security price under the Heston model is (see [18], for example) given by

$$\begin{aligned}\Phi_T^{SV}(u; r, q, \kappa, \gamma, \theta, V_0, \rho, S_0) &= \exp[iu(\log(S_0) + (r - q)T)] \\ &\quad \times \exp[\theta\kappa\gamma^{-2}((\kappa - \rho\gamma ui - d)T - 2\log((1 - g\exp(-dT))/(1 - g)))] \\ &\quad \times \exp[V_0\gamma^{-2}(\kappa - \rho\gamma ui - d)(1 - \exp(-dT))/(1 - g\exp(-dT))]\end{aligned}\quad (33)$$

where $d := \sqrt{(\rho\gamma ui - \kappa)^2 + \gamma^2(iu + u^2)}$ and $g := (\kappa - \rho\gamma ui - d)/(\kappa - \rho\gamma ui + d)$.

The Bates Model: The characteristic function of the log-security price under the SVJ model is

$$\begin{aligned}\Phi_T^{SVJ}(u; r, q, \kappa, \gamma, \theta, V_0, \rho, S_0, \lambda, a, b) &= \Phi_T^{SV}(u; r, q, \kappa, \gamma, \theta, V_0, \rho, S_0) \times \exp(-\lambda m i u T) \\ &\quad \times \exp\left[\lambda T \left(\exp\left(a i u - \frac{b^2 u^2}{2}\right) - 1\right)\right].\end{aligned}\quad (34)$$

where $m := \exp\left(a + \frac{b^2}{2}\right) - 1$.

BN-S Model: The characteristic function of the log-security price under the BNS model is

$$\begin{aligned}\Phi_T^{BNS}(u; r, q, a, b, V_0, \lambda, \rho, S_0) &= \exp[iu(\log(S_0) + (r - q - a\lambda\rho(b - \rho)^{-1})T)] \\ &\quad \times \exp[-\lambda^{-1}(u^2 + ui)(1 - \exp(-\lambda T))V_0/2] \\ &\quad \times \exp\left[a(b - f_2)^{-1}\left(b\log\left(\frac{b - f_1}{b - ui\rho}\right) + f_2\lambda T\right)\right]\end{aligned}\quad (35)$$

where

$$\begin{aligned}f_1 &= f_1(u) = ui\rho - \lambda^{-1}(u^2 + ui)(1 - \exp(-\lambda T))/2 \\ f_2 &= f_2(u) = ui\rho - \lambda^{-1}(u^2 + ui)/2.\end{aligned}$$

B The SVCJ Model

Following Duffie et al [7] we can use the SVCJ model to price options on the underlying ETF. Indeed the characteristic function of the log-ETF price under the SVCJ model is given by

$$\Phi_T^{SVCJ}(u; r, q, \kappa, \gamma, \theta, V_0, \rho, S_0, \lambda, a, b, \rho_J, \mu_v) = \exp(A(0, T, u) + iu\log(S_0) + C(0, T, u)V_0) \quad (36)$$

where

$$C(t, T, u) = -\frac{a_1(1 - e^{-a_4\tau})}{2a_4 - (a_2 + a_4)(1 - e^{-a_4\tau})}$$

$$\text{and } A(t, T, u) = A_0(t, T, u) - \lambda\tau(1 + m i u) + \lambda \exp\left(iau - \frac{b^2 u^2}{2}\right) A_1(t, T, u)$$

where $a_1 = iu(1 - iu)$, $a_2 = i\gamma\rho u - \kappa$, $a_3 = 1 - i\rho_J\mu_v u$, $a_4 = \sqrt{a_2^2 + a_1\gamma^2}$, $\tau = T - t$ and

$$A_0(t, T, u) = i(r - q)u\tau - \kappa\theta\left(\frac{a_2 + a_4}{\gamma^2}\tau + \frac{2}{\gamma^2}\log\left[1 - \frac{a_2 + a_4}{2a_4}(1 - e^{-a_4\tau})\right]\right),$$

$$A_1(t, T, u) = \frac{a_4 - a_2}{(a_4 - a_2)a_3 + \mu_v a_1}\tau - \frac{2\mu_v a_1}{(a_3 a_4)^2 - (a_2 a_3 - \mu_v a_1)^2}\log\left[1 - \frac{(a_2 + a_4)a_3 - \mu_v a_1}{2a_3 a_4}(1 - e^{-a_4\tau})\right].$$

B.1 The Bivariate Exponential Distribution

The bivariate exponential (BVE) distribution is a bivariate distribution with exponential marginals. It has joint density

$$f(x, y) = \begin{cases} \lambda_2(\lambda_1 + \lambda_{12})\bar{F}(x, y), & x > y, \\ \lambda_1(\lambda_2 + \lambda_{12})\bar{F}(x, y), & x < y \end{cases}$$

where

$$\bar{F}(s, t) := P(X > s, Y > t) = \exp[-\lambda_1 s - \lambda_2 t - \lambda_{12} \max(s, t)], \quad s, t > 0. \quad (37)$$

The marginal distribution functions then satisfy $\bar{F}_1(x) = e^{-(\lambda_1 + \lambda_{12})x}$ and $\bar{F}_2(y) = e^{-(\lambda_2 + \lambda_{12})y}$, and we write $(X, Y) \sim \text{BVE}(\lambda_1, \lambda_2, \lambda_{12})$. The characteristic function for the BVE is given by

$$\int_0^\infty \int_0^\infty e^{isx + ity} dF(x, y) = \frac{(\lambda - is - it)(\lambda_1 + \lambda_{12})(\lambda_2 + \lambda_{12}) + st\lambda_{12}}{(\lambda - is - it)(\lambda_1 + \lambda_{12} - is)(\lambda_2 + \lambda_{12} - it)} \quad (38)$$

where $\lambda := \lambda_1 + \lambda_2 + \lambda_{12}$. Using (38) we can calculate the joint characteristic function of \hat{X} in (40) to obtain

$$\begin{aligned} \Phi_{\hat{X}}(u_1, u_2; a, b, \lambda_1, \lambda_2, \lambda_{12}) &= \mathbb{E}[\exp((N - E_1)iu_1 + E_2iu_2)] \\ &= \mathbb{E}[\exp(Niu_1)] \cdot \mathbb{E}[\exp(E_1(-iu_1) + E_2(iu_2))] \\ &= \exp\left(aiau_1 - \frac{1}{2}b^2u_1^2\right) \cdot \frac{(\lambda + iu_1 - iu_2)(\lambda_1 + \lambda_{12})(\lambda_2 + \lambda_{12}) - u_1u_2\lambda_{12}}{(\lambda + iu_1 - iu_2)(\lambda_1 + \lambda_{12} + iu_1)(\lambda_2 + \lambda_{12} - iu_2)}. \end{aligned} \quad (39)$$

B.2 The Jump Approximation for the SVCJ Model

The goal here is to approximate $X := (X_1, X_2)$ as defined in (31) with

$$\hat{X} := (N - E_1, E_2) \quad (40)$$

where $N \sim N(a, b)$ and $(E_1, E_2) \sim \text{BVE}(\lambda_1, \lambda_2, \lambda_{12})$ have a bivariate exponential distribution (see [16]) that is independent of N . We therefore have five distributional parameters $(a, b, \lambda_1, \lambda_2, \lambda_{12})$ that we can choose in approximating X . Using the bivariate exponential distribution also allows us to approximate the variance jumps as well as the correlation between the two components of X in (31). If our jump approximation $\hat{X} = (N - E_1, E_2)$ is reasonably accurate, we would expect to

have¹⁵

$$\begin{aligned}
\mathbb{E}(X_1) &\approx \mathbb{E}(N - E_1) \\
&= a - \frac{1}{\lambda_1 + \lambda_{12}} \\
&=: k_1, \\
\mathbb{E}(X_2) &\approx \mathbb{E}(E_2) \\
&= \frac{1}{\lambda_2 + \lambda_{12}} \\
&=: k_2, \\
\mathbb{E}(X_1^2) &\approx \mathbb{E}((N - E_1)^2) \\
&= \mathbb{E}(N^2 - 2NE_1 + E_1^2) \\
&= (a^2 + b^2) - \frac{2a}{\lambda_1 + \lambda_{12}} + \frac{2}{(\lambda_1 + \lambda_{12})^2} \\
&=: k_3, \\
\mathbb{E}(X_1 X_2) &\approx \mathbb{E}((N - E_1)E_2) \\
&= \mathbb{E}(NE_2 - E_1 E_2) \\
&= \frac{a}{\lambda_2 + \lambda_{12}} - \frac{1}{\lambda_1 + \lambda_2 + \lambda_{12}} \left(\frac{1}{\lambda_1 + \lambda_{12}} + \frac{1}{\lambda_2 + \lambda_{12}} \right) \\
&=: k_4, \\
\mathbb{E}(X_1^3) &\approx \mathbb{E}((N - E_1)^3) \\
&= \mathbb{E}(N^3 - 3N^2 E_1 + 3NE_1^2 - E_1^3) \\
&= (a^3 + 3ab^2) - \frac{3(a^2 + b^2)}{\lambda_1 + \lambda_{12}} + \frac{6a}{(\lambda_1 + \lambda_{12})^2} - \frac{6}{(\lambda_1 + \lambda_{12})^3} \\
&=: k_5.
\end{aligned}$$

We therefore solve¹⁶ the following optimization problem

$$\begin{aligned}
&\min_{a, b, \lambda_1, \lambda_2, \lambda_{12}} && (\mathbb{E}(X_1) - k_1)^2 + (\mathbb{E}(X_2) - k_2)^2 + (\mathbb{E}(X_1^2) - k_3)^2 + (\mathbb{E}(X_1 X_2) - k_4)^2 \\
&&& + (\mathbb{E}(X_1^3) - k_5)^2 \\
&\text{subject to} && b, \lambda_1, \lambda_2, \lambda_{12} \geq 0.
\end{aligned} \tag{41}$$

We note that the optimization problem (41) is not convex and so we are only guaranteed to find local minima when we solve it. This was never a problem in the numerical experiments of Section 7. For the SSO and SDS LETFs of Section D, however, we needed to resolve (41) once from a new starting point in order to obtain a sufficiently good fit. We note that it would be easy to automate the process of seeking a good starting point, resolving (41) and repeating these two steps until the objective function in (41) is sufficiently small.

After solving (41) we then use \hat{X} rather than X when modeling the dynamics of L_t . In order to

¹⁵We note that $\mathbb{E}(E_1^n) = \frac{n!}{(\lambda_1 + \lambda_{12})^n}$, $\mathbb{E}(E_2^n) = \frac{n!}{(\lambda_2 + \lambda_{12})^n}$ and $\mathbb{E}(E_1 E_2) = \frac{1}{\lambda_1 + \lambda_2 + \lambda_{12}} \left(\frac{1}{\lambda_1 + \lambda_{12}} + \frac{1}{\lambda_2 + \lambda_{12}} \right)$ and used these expressions in our calculations.

¹⁶As we don't have analytic expressions for $\mathbb{E}(X_1), \mathbb{E}(X_2), \mathbb{E}(X_1^2), \mathbb{E}(X_1 X_2), \mathbb{E}(X_1^3)$, we simply estimated them using Monte-Carlo.

maintain the martingale property of these dynamics, however, we replace m_L in (28) with

$$\begin{aligned}\hat{m} &:= -p^* + (1-p^*) \cdot \mathbb{E}[\exp(N - E_1) - 1] \\ &= -p^* + (1-p^*) \left(\exp\left(a^* + \frac{1}{2}b^{*2}\right) \frac{\lambda_1^* + \lambda_{12}^*}{1 + \lambda_1^* + \lambda_{12}^*} - 1 \right).\end{aligned}\quad (42)$$

where $(a^*, b^*, \lambda_1^*, \lambda_2^*, \lambda_{12}^*)$ is the optimal solution to (41). The characteristic function, $\Phi_{\hat{X}}(\cdot)$, of \hat{X} is easily computed (see Appendix B.1) which means we can employ the approach of Duffie et al. [7] to compute the characteristic function of the log-LETF price conditional on $N_1(T) = 0$. This characteristic function may then be used with the Carr-Madan [5] approach to approximate $\hat{C}(L_0, K, T)$.

B.3 The Characteristic Function of the Approximated log-LETF Price

The characteristic function of the approximated log-LETF price conditional on $N_1(T) = 0$ is given by

$$\hat{\Phi}_L^{N_1=0}(u; \phi, r, q, f, \kappa, \gamma, \theta, V_0, \rho, L_0, \lambda, a, b, \rho_J, \mu_v) = \exp(\hat{A}(0, T, u) + \hat{B}(0, T, u) \log(L_0) + \hat{C}(0, T, u) V_0^L)$$

where $\hat{A}, \hat{B}, \hat{C}$ satisfy the following ODEs¹⁷:

$$\begin{aligned}\frac{d\hat{B}}{dt} &= 0, \\ \frac{d\hat{C}}{dt} &= -\frac{1}{2}\hat{B}^2 - \hat{B}\hat{C}\rho_L\gamma_L - \frac{1}{2}\hat{C}^2\gamma_L^2 + \frac{1}{2}\hat{B} + \kappa_L\hat{C}, \\ \frac{d\hat{A}}{dt} &= -(r - q_L - \lambda\hat{m})\hat{C} - \kappa_L\theta_L\hat{B} + \lambda_L - \lambda_L \cdot \Phi_{\hat{X}}(u, \hat{B}; \hat{a}, \hat{b}, \lambda_1, \lambda_2, \lambda_{12}),\end{aligned}$$

with boundary conditions $\hat{B}(T, T, u) = iu$, $\hat{C}(T, T, u) = 0$ and $\hat{A}(T, T, u) = 0$, and where

$$(q_L, \kappa_L, \gamma_L, \theta_L, V_0^L, \rho_L, L_0, \lambda_L, \hat{a}, \hat{b}, \lambda_1, \lambda_2, \lambda_{12}) := (\phi q + f, \kappa, |\phi|\gamma, \phi^2\theta, \phi^2V_0, \text{sign}(\phi)\rho, L_0, \lambda(1-p^*), a^*, b^*, \lambda_1^*, \lambda_2^*, \lambda_{12}^*).$$

Note that \hat{m} and $\Phi_{\hat{X}}$ are specified in equations (42) and (39). We solved these ODEs and they have the following explicit solution:

$$\begin{aligned}\hat{B}(t, T, u) &= iu, \\ \hat{C}(t, T, u) &= -\frac{\hat{a}_1(1 - e^{-\hat{a}_3\tau})}{2\hat{a}_3 - (\hat{a}_2 + \hat{a}_3)(1 - e^{-\hat{a}_3\tau})}, \\ \hat{A}(t, T, u) &= \hat{A}_0(t, T, u) - \lambda\tau(1 + \hat{m}iu) + \lambda_L \exp\left(\hat{a}iu - \frac{\hat{b}^2u^2}{2}\right) \hat{A}_1(t, T, u),\end{aligned}$$

where $\hat{a}_1 = iu(1 - iu)$, $\hat{a}_2 = \gamma_L\rho_L iu - \kappa_L$, $\hat{a}_3 = \sqrt{\hat{a}_2^2 + \hat{a}_1\gamma_L^2}$, $\tau = T - t$,

$$\alpha(x) = \frac{\hat{a}_3 - \hat{a}_2}{x(\hat{a}_3 - \hat{a}_2) + \hat{a}_1}\tau - \frac{2\hat{a}_1}{(x\hat{a}_3)^2 - (x\hat{a}_3 - \hat{a}_1)^2} \log\left[1 - \frac{(\hat{a}_2 + \hat{a}_3)x - \hat{a}_1}{2\hat{a}_3}(1 - e^{-\hat{a}_3\tau})\right]$$

¹⁷See Duffie et al [7] for the derivation of these ODEs.

and

$$\begin{aligned}\hat{A}_0(t, T, u) &= i(r - q_L)u\tau - \kappa_L\theta_L \left(\frac{\hat{a}_2 + \hat{a}_3}{\gamma_L^2}\tau + \frac{2}{\gamma_L^2} \log \left[1 - \frac{\hat{a}_2 + \hat{a}_3}{2\hat{a}_3}(1 - e^{-\hat{a}_3\tau}) \right] \right), \\ \hat{A}_1(t, T, u) &= \alpha(\lambda_2 + \lambda_{12}) \cdot \frac{\lambda_2 + \lambda_{12}}{(\lambda_1 + \lambda_{12} + iu)(\lambda_1 + iu)} [(\lambda_1 + \lambda_{12})(\lambda_1 + iu) + iu\lambda_{12}] \\ &\quad - \alpha(\lambda_1 + \lambda_2 + \lambda_{12} + iu) \cdot \frac{iu\lambda_{12}(\lambda_1 + iu)}{(\lambda_1 + \lambda_{12} + iu)(\lambda_1 + iu)}.\end{aligned}$$

C Additional Numerical Results

C.1 Jump Approximation Parameters for the SVCJ Model

We report here the jump approximation parameters for the SVCJ model that we obtained from solving the optimization problem of Appendix B.2. These parameter values were used to obtain C_{tran} for the SVCJ model in Section 7 (parameter sets II and III) and Appendix C.2 (parameter set I).

Table 12: Optimized Jump Approximation Parameters for the SVCJ Model

Parameter Set	Leverage Ratio	<u>SVCJ model</u>				
		a^*	b^*	λ_1^*	λ_2^*	λ_{12}^*
I	2	0.0641	0.2114	0.9571	17.3016	7.4705
	3	0.2524	0.1910	0.1112	8.6678	2.6477
	-1	0.0484	0.1113	0.1112	59.6036	23.4571
	-2	0.1315	0.2163	0.2282	14.9813	6.9231
	-3	0.4228	0	0.0193	9.1694	2.1501
II	2	0.2225	0.5919	0.8507	2.5896	0.1404
	3	0.5192	0.6608	0.8826	1.1648	0.0719
	-1	0.6063	0.0009	0	8.5916	2.1552
	-2	0.9422	0	1.5352	2.5810	0
	-3	1.2021	0.0003	1.3639	1.1316	0
III	2	0.0204	0.4170	1.0564	6.7329	0
	3	0.1580	0.5781	0.9774	2.9885	0
	-1	0.3766	0	0	12.3884	6.3770
	-2	0.8057	0	2.0278	6.6275	0
	-3	1.0509	0	1.6341	2.9142	0

C.2 Results for Parameter Set I

We report in Tables 13 to 15 our numerical results for the low-volatility environment of parameter set I. We see that there is very little variation in LETF option prices and implied volatilities across

the three models. In addition, the Monte-Carlo prices are very close to the prices obtained via numerical transform inversion for each model.

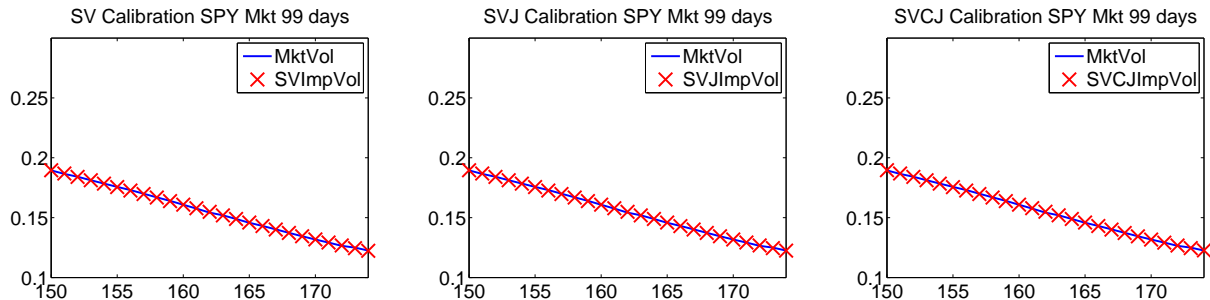
D Calibration to Market Data

The focus of this paper has been on model-consistent pricing of ETF and LETF options. While not our main focus, it is also of interest to see how the LETF option prices generated by these (calibrated) models compare with the corresponding LETF option prices in the market-place. In this appendix we perform such a study using **Bloomberg** price data as of the market close on June 14th, 2013. We emphasize that the observations we make only apply to the market data as of that date and that a more thorough¹⁸ empirical study would be required to investigate how these models perform across time and different market regimes.

We took the SPDR S&P 500 ETF (ticker SPY) as our underlying security and considered 3-month options on the corresponding¹⁹ double long, double short, triple long and triple short LETFs. The underlying price at the close was 163.18, the 3-month call option strikes ranged from 150 to 174 and the ATM volatility was approximately 15.2%. The 3-month risk-free rate was 0.29%. According to **Bloomberg** the dividend yield for the underlying ETF was 1.63%. Rather than using this value and the LETF dynamics in (4) to determine the dividend yields of the LETFs we again used the dividend yields provided by **Bloomberg**. These yields were 0.06% and .03% for SSO and UPRO, respectively. The inverse LETFs, SDS and SPXU, do not pay dividends and therefore have dividend yields of zero.

In calibrating the SV, SVJ and SVCJ models we again fixed the parameter ρ and determined the remaining parameters by minimizing the sum-of-squares between the market implied volatilities and the model's implied volatilities. Table 16 displays the calibrated parameters for the three models while Figure 2 displays the market and model implied volatility skews on the calibration date. Table 17 also reports the calibration performance for the three models in terms of pricing error and implied volatility error. We see that the calibration was successful for each model with any pricing error well inside the bid-offer spread we would expect to see in the market.

Figure 2: Volatility skews for SPY options



¹⁸We also investigated how the model performed on June 30th, 2013 and obtained similar results.

¹⁹With tickers SSO, SDS, UPRO and SPXU, respectively. Note also that all options had 99 days to-maturity rather than exactly 3 months.

Table 13: Option prices on underlying index / ETF for parameter set I computed via Monte-Carlo and transform inversion approaches. Approximate 95% confidence intervals are reported in brackets.

Moneyiness	BS vol(%)	BS price	Option price (SV)		Option price (SVJ)		Option price (SVCJ)	
$\frac{K}{S_0}$	Σ_{BS}	C_{BS}	C_{sim}	C_{tran}	C_{sim}	C_{tran}	C_{sim}	C_{tran}
0.85	21.47	16.37	16.38	16.38	16.37	16.37	16.37	16.37
			[16.38, 16.38]	-	[16.37, 16.37]	-	[16.37, 16.37]	-
1	20.17	5.92	5.99	5.99	5.92	5.92	5.94	5.94
			[5.99, 5.99]	-	[5.92, 5.92]	-	[5.94, 5.94]	-
1.15	19.20	1.23	1.27	1.27	1.22	1.22	1.23	1.23
			[1.27, 1.27]	-	[1.22, 1.22]	-	[1.23, 1.23]	-

Table 14: Comparison of Black-Scholes implied-volatilities: parameter set I

Leverage ratio	Moneyiness		Implied Volatility (SV)			Implied Volatility (SVJ)			Implied Volatility (SVCJ)		
ϕ	$\frac{K_S}{S_0}$	$\frac{K_L}{L_0}$	Σ_S	Σ_L	$\frac{\Sigma_L}{\Sigma_S}$	Σ_S	Σ_L	$\frac{\Sigma_L}{\Sigma_S}$	Σ_S	Σ_L	$\frac{\Sigma_L}{\Sigma_S}$
2	0.85	0.7	21.51	43.11	2.00	21.43	43.14	2.01	21.43	43.21	2.02
	1	1	20.41	40.66	1.99	20.17	40.22	1.99	20.22	40.33	1.99
	1.15	1.3	19.44	38.82	2.00	19.18	38.26	1.99	19.24	38.41	2.00
3	0.85	0.55		64.92	3.02		65.48	3.06		65.22	3.04
	1	1		60.79	2.98		60.26	2.99		60.27	2.98
	1.15	1.45		58.17	2.99		57.30	2.99		57.48	2.99
-1	0.85	1.15		21.43	1.00		21.20	0.99		21.25	0.99
	1	1		20.49	1.00		20.21	1.00		20.28	1.00
	1.15	0.85		19.39	1.00		19.27	1.00		19.25	1.00
-2	0.85	1.3		42.91	1.99		42.38	1.98		42.51	1.98
	1	1		41.16	2.02		40.60	2.01		40.75	2.02
	1.15	0.7		38.77	1.99		38.81	2.02		38.64	2.01
-3	0.85	1.45		64.45	3.00		63.59	2.97		63.82	2.98
	1	1		62.00	3.04		61.18	3.03		61.40	3.04
	1.15	0.55		58.04	2.99		58.82	3.07		58.24	3.03

Table 15: Comparing leveraged ETFs option prices with approximate prices in parameter set I. Approximate 95% confidence intervals are reported in brackets.

Leverage ratio	Moneyness		Option price (SV)		Option price (SVJ)		Option price (SVCJ)	
	ϕ	$\frac{K_S}{S_0}$ $\frac{K_L}{L_0}$	C_{sim}	C_{tran}	C_{sim}	C_{tran}	C_{sim}	C_{tran}
2	0.85	0.7	31.81	31.80	31.81	31.81	31.82	31.79
			[31.80, 31.81]	-	[31.80, 31.81]	-	[31.81, 31.82]	-
	1	1	11.65	11.65	11.53	11.53	11.56	11.55
			[11.65, 11.66]	-	[11.53, 11.54]	-	[11.56, 11.57]	-
	1.15	1.3	2.91	2.91	2.80	2.80	2.83	2.84
			[2.91, 2.91]	-	[2.79, 2.80]	-	[2.82, 2.83]	-
3	0.85	0.55	46.75	46.74	46.80	46.79	46.78	46.76
			[46.74, 46.76]	-	[46.79, 46.81]	-	[46.77, 46.78]	-
	1	1	17.23	17.21	17.08	17.07	17.08	17.05
			[17.22, 17.23]	-	[17.07, 17.09]	-	[17.08, 17.09]	-
	1.15	1.45	4.98	4.98	4.79	4.79	4.83	4.81
			[4.97, 4.98]	-	[4.78, 4.79]	-	[4.82, 4.83]	-
-1	0.85	1.15	1.66	1.66	1.61	1.61	1.62	1.64
			[1.66, 1.66]	-	[1.61, 1.61]	-	[1.62, 1.62]	-
	1	1	6.01	6.01	5.93	5.93	5.95	5.96
			[6.01, 6.02]	-	[5.93, 5.94]	-	[5.95, 5.96]	-
	1.15	0.85	16.10	16.10	16.09	16.08	16.08	16.08
			[16.10, 16.10]	-	[16.08, 16.09]	-	[16.08, 16.08]	-
-2	0.85	1.3	3.78	3.80	3.67	3.67	3.69	3.76
			[3.78, 3.78]	-	[3.66, 3.67]	-	[3.69, 3.70]	-
	1	1	11.79	11.79	11.64	11.63	11.68	11.72
			[11.79, 11.80]	-	[11.63, 11.64]	-	[11.67, 11.68]	-
	1.15	0.7	31.34	31.33	31.35	31.33	31.33	31.33
			[31.34, 31.35]	-	[31.34, 31.35]	-	[31.32, 31.34]	-
-3	0.85	1.45	6.43	6.46	6.23	6.24	6.28	6.31
			[6.43, 6.44]	-	[6.22, 6.23]	-	[6.28, 6.29]	-
	1	1	17.56	17.55	17.33	17.31	17.39	17.41
			[17.55, 17.56]	-	[17.33, 17.34]	-	[17.39, 17.40]	-
	1.15	0.55	46.22	46.20	46.27	46.25	46.23	46.25
			[46.21, 46.22]	-	[46.26, 46.28]	-	[46.22, 46.24]	-

Table 16: Calibrated Model Parameters

Parameters	SV Model	SVJ Model	SVCJ Model
Risk free rate r	0.0029	0.0029	0.0029
Speed of mean reversion κ	4.5858	2.7509	6.3404
Volatility of variance γ	0.6284	0.5498	0.7197
Long run mean variance θ	0.0279	0.0270	0.0230
Initial variance V_0	0.0279	0.0270	0.0230
Correlation ρ	-0.7571	-0.7571	-0.82
Jump arrival rate λ	n/a	1.0926	1.7665
m	n/a	-0.0252	-0.0121
b	n/a	0.0100	0.0411
μ_v	n/a	n/a	0.0117
ρ_J	n/a	n/a	-0.6917

Table 17: Market prices and implied volatilities for SPY options versus corresponding calibrated model prices and model implied volatilities. Root-mean-squared errors (RMSE) are reported in the final row.

Moneyness	Implied Volatility(%)				Option Price			
	Mkt ImpVol	SV ImpVol	SVJ ImpVol	SVCJ ImpVol	Mkt Price	SV Price	SVJ Price	SVCJ Price
$\frac{K}{S_0}$	Σ_{mkt}	Σ_{SV}	Σ_{SVJ}	Σ_{SVCJ}	C_{mkt}	C_{SV}	C_{SVJ}	C_{SVCJ}
0.919	18.95	18.96	18.96	18.97	21.00	20.97	20.93	21.01
0.925	18.65	18.68	18.68	18.69	20.09	20.05	20.02	20.08
0.932	18.42	18.41	18.41	18.41	19.16	19.14	19.12	19.17
0.938	18.12	18.12	18.13	18.12	18.25	18.24	18.22	18.26
0.944	17.84	17.84	17.84	17.84	17.37	17.35	17.34	17.36
0.950	17.57	17.55	17.56	17.55	16.46	16.47	16.46	16.46
0.956	17.30	17.26	17.27	17.26	15.57	15.59	15.59	15.58
0.962	17.00	16.97	16.97	16.97	14.72	14.73	14.73	14.71
0.968	16.69	16.68	16.68	16.68	13.85	13.87	13.89	13.85
0.974	16.41	16.38	16.38	16.38	13.00	13.03	13.05	13.00
0.981	16.08	16.09	16.09	16.09	12.17	12.20	12.23	12.17
0.987	15.76	15.79	15.79	15.79	11.36	11.38	11.41	11.35
0.993	15.42	15.49	15.49	15.49	10.56	10.58	10.62	10.54
0.999	15.20	15.19	15.19	15.19	9.76	9.79	9.83	9.76
1.005	14.89	14.89	14.89	14.89	3.25	3.23	3.19	3.26
1.011	14.57	14.60	14.59	14.60	2.77	2.75	2.70	2.78
1.017	14.31	14.30	14.30	14.30	2.34	2.32	2.26	2.35
1.023	14.03	14.01	14.01	14.01	1.95	1.93	1.87	1.95
1.030	13.73	13.73	13.72	13.72	1.61	1.58	1.54	1.60
1.036	13.45	13.45	13.45	13.44	1.30	1.29	1.25	1.29
1.042	13.18	13.18	13.18	13.17	1.04	1.03	1.01	1.03
1.048	12.92	12.92	12.92	12.91	0.82	0.82	0.82	0.81
1.054	12.65	12.68	12.68	12.68	0.64	0.64	0.66	0.63
1.060	12.49	12.45	12.46	12.46	0.49	0.50	0.53	0.49
1.066	12.25	12.24	12.25	12.27	0.38	0.39	0.43	0.39
RMSE		0.02	0.02	0.03		0.01	0.01	0.01

Table 18: Optimized jump approximation parameters in the SVCJ model

Ticker	Leverage Ratio	<u>SVCJ model</u>					
		ϕ	a^*	b^*	λ_1^*	λ_2^*	λ_{12}^*
SSO	2		0.0390	0.0050	3.9575	10.1292	10.8609
SDS	-2		0.1156	0.0311	0.0095	12.3115	10.5301
UPRO	3		0.0788	0.0001	3.5849	5.0906	4.4631
SPXU	-3		0.1453	0	4.8540	5.7947	3.7325

In the case of the calibrated SVCJ model, we first had to solve for the optimal jump distribution approximations for the four different leverage ratios. The optimal parameters are reported in Table 18. We then computed the calibrated model prices and implied volatilities of European call options on the LETFs and compared them with their corresponding market prices and implied volatilities. These prices are reported in Tables 19 to 22 for SSO (double long), SDS (double short), UPRO (triple long) and SPXU (triple short), respectively, and for different values of money-ness.

We note that for each model-ETF combination, the root-mean-squared pricing error is relatively small and typically within the (non-reported) bid-ask price ranges that we see in the market. On the date in question at least, we can conclude that all three calibrated models are capable of reproducing market prices of ETF options. We also note, however, that the current market regime could be characterized as a low-volatility regime (compare Figure 2 with the low-volatility graphs in Figure 1) and so it is not surprising given the results in Table 15 that the ETF option prices broadly agree across all three models. In contrast, the results in Tables 4 and 5 suggest that we would expect considerably less agreement among the three models in a high volatility regime.

We might also conclude that in the current low-volatility environment, market participants could use any of the three models to hedge an ETF-ETF option portfolio by trading in the underlying ETF only rather than in the leveraged ETF. This might be preferable as the underlying ETF typically has a lower bid-offer spread than the corresponding LETFs. This of course also allows the possibility of combining an ETF options trading book with ETF options trading books and risk-managing them together rather than separately. That said, we do acknowledge that a more rigorous study would be required before we would recommend risk-managing such portfolios using these models. Moreover, in a high volatility environment we expect that only one of our three models might be suitable for hedging.

More specific observations can also be made. We note that the pricing error is generally smaller for the negative LETFs than for the positive LETFs on the date in question. The root-mean-squared pricing error for the negative LETFs is less than 7 cents in all three models whereas the corresponding number for the positive LETFs is 15 cents. We also observe that the implied volatility ratios (the ratios of implied volatilities of the ETF to the corresponding implied volatilities of the underlying ETF) are generally close to the leverage multiple. In our particular data-set we see that the ratios for the negative LETFs are almost always higher than the ratios for the positive leverage LETFs. Consistent with this observation is the fact that the market prices of the negative

LETFs all tend to be greater than the calibrated model prices. Similarly the market prices of the positive LETFs all tend to be less than the calibrated model prices. Indeed, the market prices of the SSO (double long) options are uniformly greater than the model prices at all money-ness levels. It is quite possible that these systematic differences are due to inaccurate calibration of the forward LETF prices. As stated earlier, we simply took the dividend yields for the SSO and UPRO LETFs to be those published by **Bloomberg**. A superior approach would have been to calibrate the implied dividend yields (and borrow rates) via put-call parity. This would ensure that the implied forward rates for the various LETFs were correct. Given the relatively wide bid-offer spreads of LETF option prices, this approach would also likely have some noise although it should still yield superior model prices. (It is important to note, however, that the price differences in question are small in magnitude and almost certainly lie within the bid-ask spreads.)

Table 19: SSO (Double Long): Market Prices and Implied Volatilities Versus Calibrated Model Prices and Implied Volatilities.

Leverage ratio	Moneyess	Implied Volatility (%)						Option Price			
		Mkt ImpVol	SV Imp Vol	SVJ ImpVol	SVCJ ImpVol	Mkt Price	SV Price	SVJ Price	SVCJ Price		
ϕ	$\frac{\kappa_L}{L_0}$	Σ_L	Σ_L	Σ_L	Σ_L	C_{mkt}	C_{SV}	C_{SVJ}	C_{SVCJ}		
2	0.850	35.67	37.67	1.99	37.68	1.99	37.04	1.95	13.51	13.51	13.44
	0.862	34.95	37.06	1.98	37.07	1.98	36.44	1.95	12.45	12.68	12.61
	0.875	34.37	36.44	1.98	36.46	1.98	35.83	1.95	11.63	11.87	11.80
	0.888	34.23	35.82	2.01	35.84	2.01	35.22	1.97	10.88	11.08	11.00
	0.900	33.65	35.21	2.01	35.23	2.01	34.61	1.97	10.10	10.30	10.22
	0.913	33.15	34.59	2.00	34.61	2.00	34.01	1.97	9.35	9.55	9.47
	0.926	32.49	33.97	2.00	33.98	2.00	33.40	1.97	8.60	8.81	8.73
	0.938	32.16	33.34	2.00	33.36	2.00	32.79	1.97	7.92	8.10	8.01
	0.951	31.71	32.72	2.00	32.74	2.00	32.18	1.96	7.25	7.41	7.32
	0.964	31.09	32.10	2.00	32.12	2.00	31.57	1.96	6.58	6.74	6.66
	0.976	30.54	31.48	1.99	31.49	1.99	30.97	1.96	5.95	6.10	6.02
	0.989	30.01	30.86	1.99	30.87	1.99	30.37	1.96	5.35	5.49	5.41
	1.002	29.47	30.25	1.99	30.26	1.99	29.77	1.96	4.78	4.91	4.83
	1.014	28.98	29.64	1.99	29.64	1.99	29.17	1.96	4.25	4.36	4.28
	1.027	28.35	29.04	1.99	29.04	1.99	28.59	1.96	3.73	3.84	3.77
	1.040	27.75	28.44	1.99	28.44	1.99	28.01	1.96	3.25	3.36	3.29
RMSE	1.052	27.26	27.86	1.99	27.86	1.99	27.44	1.96	2.82	2.91	2.85
	1.065	26.73	27.28	1.99	27.29	1.99	26.89	1.96	2.42	2.50	2.44
	1.078	26.23	26.73	1.99	26.74	1.99	26.35	1.96	2.06	2.13	2.08
	1.091	25.77	26.20	1.99	26.20	1.99	25.84	1.96	1.74	1.80	1.75
	1.103	25.21	25.69	1.99	25.70	1.99	25.36	1.96	1.44	1.50	1.46
	1.116	24.77	25.20	1.99	25.22	1.99	24.91	1.96	1.19	1.24	1.21
	1.129	24.23	24.75	1.99	24.77	1.99	24.49	1.97	0.96	1.02	0.99
	1.141	23.88	24.33	1.99	24.36	1.99	24.11	1.96	0.78	0.83	0.80
		1.14	1.15	0.69	0.15	0.15	0.15	0.15	0.09		

Table 20: SDS (Double Short): Market Prices and Implied Volatilities Versus Calibrated Model Prices and Implied Volatilities.

Leverage ratio	Moneyness	Implied Volatility (%)								Option Price			
		Mkt ImpVol	SV Imp Vol	SVJ ImpVol	SVCJ ImpVol	Mkt Price	SV Price	SVJ Price	SVCJ Price				
ϕ	$\frac{K_L}{L_0}$	Σ_L	Σ_L	$\frac{\Sigma_L}{\Sigma_S}$	Σ_L	$\frac{\Sigma_L}{\Sigma_S}$	Σ_L	$\frac{\Sigma_L}{\Sigma_S}$	C_{mkt}	C_{SV}	C_{SVJ}	C_{SVCJ}	
-2	0.874	25.14	2.01	25.41	2.04	25.41	2.04	27.23	2.19	5.45	5.46	5.46	5.55
	0.899	26.95	2.09	26.52	2.05	26.49	2.05	27.84	2.16	4.75	4.72	4.72	4.80
	0.924	28.02	2.08	27.75	2.06	27.70	2.06	28.69	2.13	4.10	4.08	4.08	4.15
	0.949	29.58	2.11	29.02	2.07	28.97	2.07	29.68	2.12	3.57	3.53	3.52	3.58
	0.974	30.84	2.12	30.30	2.08	30.25	2.07	30.74	2.11	3.10	3.06	3.05	3.09
	0.999	32.33	2.13	31.55	2.08	31.50	2.07	31.82	2.09	2.72	2.66	2.65	2.68
	1.024	33.55	2.13	32.76	2.07	32.71	2.07	32.90	2.08	2.38	2.31	2.31	2.33
	1.049	34.61	2.11	33.92	2.07	33.87	2.07	33.95	2.07	2.08	2.02	2.02	2.03
	1.074	35.84	2.11	35.02	2.06	34.98	2.06	34.97	2.06	1.84	1.77	1.77	1.77
	1.099	36.97	2.10	36.07	2.06	36.03	2.05	35.96	2.05	1.63	1.56	1.56	1.55
RMSE	1.124	37.93	2.09	37.08	2.05	37.03	2.04	36.91	2.04	1.44	1.38	1.37	1.36
	1.149	38.92	2.09	38.03	2.04	37.99	2.03	37.82	2.02	1.28	1.22	1.21	1.20
				0.69		0.73		0.95		0.05		0.06	0.06

Table 21: UPRO (Triple Long): Market Prices and Implied Volatilities Versus Calibrated Model Prices and Implied Volatilities.

Leverage ratio	Moneyness	Implied Volatility (%)						Option Price					
		Mkt ImpVol	SV Imp Vol	SVJ ImpVol	SVCJ ImpVol	Mkt Price	SV Price	SVJ Price	SVCJ Price				
ϕ	$\frac{K_L}{L_0}$	Σ_L	$\frac{\Sigma_L}{\Sigma_S}$	Σ_L	$\frac{\Sigma_L}{\Sigma_S}$	Σ_L	$\frac{\Sigma_L}{\Sigma_S}$	Σ_L	$\frac{\Sigma_L}{\Sigma_S}$	C_{mkt}	C_{SV}	C_{SVJ}	C_{SVCJ}
3	0.772	57.67	3.04	56.56	2.98	56.59	2.98	56.35	2.97	16.80	16.71	16.71	16.69
	0.779	55.60	2.98	56.16	3.01	56.20	3.01	55.95	2.99	16.25	16.30	16.30	16.28
	0.787	54.76	2.94	55.76	2.98	55.80	2.99	55.56	2.97	15.80	15.88	15.89	15.87
	0.795	56.20	3.05	55.36	3.01	55.40	3.01	55.17	3.00	15.55	15.48	15.48	15.46
	0.802	53.02	2.88	54.96	2.99	55.01	2.99	54.78	2.98	14.90	15.07	15.08	15.06
	0.810	57.03	3.10	54.56	2.96	54.61	2.97	54.39	2.95	14.90	14.67	14.68	14.65
	0.818	56.03	3.09	54.17	2.99	54.22	2.99	54.00	2.98	14.45	14.27	14.28	14.26
	0.825	54.50	3.01	53.77	2.97	53.82	2.97	53.61	2.96	13.95	13.88	13.88	13.86
	0.833	53.99	3.03	53.38	2.99	53.43	2.99	53.22	2.98	13.55	13.49	13.49	13.47
	0.841	51.96	2.91	52.99	2.97	53.04	2.97	52.83	2.96	13.00	13.10	13.11	13.09
	0.848	51.90	2.91	52.59	2.95	52.64	2.95	52.45	2.94	12.65	12.72	12.73	12.71
	0.856	50.84	2.89	52.20	2.97	52.25	2.98	52.06	2.97	12.20	12.34	12.35	12.33
	0.864	51.16	2.91	51.81	2.95	51.86	2.95	51.68	2.94	11.90	11.97	11.98	11.96
	0.879	49.82	2.88	51.03	2.96	51.08	2.96	50.92	2.95	11.10	11.24	11.24	11.22
	0.917	48.85	2.93	49.10	2.94	49.15	2.95	49.02	2.94	9.45	9.48	9.49	9.47
RMSE	0.955	46.80	2.91	47.19	2.93	47.23	2.94	47.16	2.93	7.80	7.85	7.86	7.85
	0.993	44.10	2.86	45.32	2.93	45.36	2.93	45.32	2.93	6.20	6.37	6.37	6.37
	1.032	42.51	2.86	43.50	2.92	43.53	2.92	43.54	2.92	4.90	5.03	5.04	5.04
	1.070	41.20	2.88	41.75	2.92	41.77	2.92	41.83	2.92	3.80	3.87	3.88	3.88
	1.108	40.18	2.99	40.09	2.98	40.11	2.98	40.21	2.99	2.90	2.89	2.89	2.90
	1.146	37.99	2.94	38.54	2.98	38.57	2.98	38.73	3.00	2.02	2.08	2.09	2.10
	1.184	37.12	2.97	37.15	2.98	37.19	2.99	37.42	3.00	1.45	1.45	1.46	1.48
	1.223	35.92	2.93	35.94	2.94	36.00	2.94	36.32	2.96	0.98	0.98	0.99	1.01
			1.06		1.07		1.09		0.11		0.11	0.11	

Table 22: SPXU (Triple Short): Market Prices and Implied Volatilities Versus Calibrated Model Prices and Implied Volatilities.

Leverage ratio	Moneyness	Implied Volatility (%)						Option Price			
		Mkt ImpVol	SV Imp Vol	SVJ ImpVol	SVCJ ImpVol	Mkt Price	SV Price	SVJ Price	SVCJ Price		
ϕ	$\frac{K_L}{L_0}$	Σ_L	Σ_L	$\frac{\Sigma_L}{\Sigma_S}$	Σ_L	$\frac{\Sigma_L}{\Sigma_S}$	Σ_L	$\frac{\Sigma_L}{\Sigma_S}$	Σ_L	C_{mkt}	C_{SV}
-3	0.797	35.40	2.89	37.75	3.09	37.78	3.08	38.89	3.17	5.05	5.10
	0.839	38.44	2.97	39.62	3.07	39.58	3.06	39.99	3.10	4.30	4.34
	0.881	42.16	3.14	41.76	3.10	41.67	3.10	41.58	3.09	3.70	3.68
	0.923	44.21	3.15	43.98	3.14	43.88	3.13	43.44	3.10	3.15	3.14
	0.965	46.40	3.18	46.18	3.16	46.08	3.16	45.38	3.11	2.70	2.69
	1.007	48.95	3.17	48.29	3.12	48.19	3.11	47.32	3.05	2.35	2.32
	1.049	50.52	3.14	50.28	3.13	50.19	3.12	49.19	3.06	2.02	2.01
	1.091	52.16	3.13	52.15	3.13	52.07	3.12	50.98	3.06	1.75	1.75
	1.133	54.29	3.09	53.91	3.07	53.82	3.07	52.69	3.00	1.55	1.53
	1.175	55.59	3.07	55.56	3.07	55.47	3.06	54.30	3.00	1.35	1.34
RMSE	1.217	57.29	3.07	57.10	3.06	57.01	3.05	55.83	2.99	1.20	1.19
				0.85		0.88		1.62		0.02	0.03
											0.06